Article:
Fonnesu, M, Felletti, F, Haughton, PDW et al. (2018) Hybrid event bed character and processes linked to turbidite system sub-environments: the North Apennine Gottero Sandstone (north-west Italy). Sedimentology, 65 (1). pp. 151-190. ISSN: 0037-0746

https://doi.org/10.1111/sed.12376

Hybrid event bed character and distribution linked to turbidite system sub-environments: the North Apennine Gottero Sandstone (NW Italy)

MARCO FONNESU*,†, FABRIZIO FELLETTI†, PETER D.W. HAUGHTON*, MARCO PATACCI‡ and WILLIAM D. McCAFFREY‡

* *UCD School of Earth Sciences, University College Dublin, Belfield, Dublin 4, Ireland (E-mail: marco.fonnesu@ucd.connect.ie)*

† *Dipartimento di Scienze della Terra, Università degli Studi di Milano, Via Mangiagalli 34, 20034 Milano, Italy*

‡ *Turbidites Research Group, School of Earth and Environment, University of Leeds, Leeds LS2 9JT, UK*

Mail id: marco.fonnesu@ucd.connect.ie

Keywords: turbidites, hybrid event beds, facies tract, deep-water fan, confined basin, sediment gravity flows, lobes, Apennines.

Abstract

This study documents the character and occurrence of hybrid event beds (HEBs) deposited across a range of deep-water sub-environments in the Cretaceous-Palaeocene Gottero system, NW Italy. Detailed fieldwork (>5200 m of sedimentary logs) has shown that HEBs are most abundant in the distal confined basin plain domain (>31% of total thickness). In more proximal sectors, HEBs occur within outer-fan and mid-fan lobes (up to 15% of total thickness), whereas they are not observed in the inner-fan channelised area. Six HEB types (HEB-1 to 6) were differentiated mainly on basis of the texture of their muddier and chaotic central division (H3). The confined basin plain sector is dominated by thick (max 9.57 m; average 2.15 m) and tabular HEBs (HEB-1 to 4). Their H3 division can include very large substrate slabs, evidence of extensive auto-injection and clast break-up, and abundant mudstone clasts set in a sandy matrix (dispersed clay ~20%). These beds are thought to have been generated by highly energetic flows capable of delaminating the sea-floor

locally, and carrying large rip-up clasts for relatively short distances before arresting. The unconfined lobes of the mid-fan sector are dominated by thinner (average 0.38 m) HEBs (HEB-5 and 6). Their H3 divisions are characterised by floating mudstone clasts and clay-enriched matrices (dispersed clay >25%) with hydraulically-fractionated components (mica, organic matter, clay flocs). These HEBs are thought to have been deposited by less energetic flows that underwent early turbulence damping following incorporation of mud at proximal locations and by segregation during transport. Although there is a tendency to look to external factors to account for hybrid event bed development, systems like the Gottero imply intrabasinal factors can also be important; specifically the type of substrate available (muddy or sandy) and where and how erosion is achieved across the system producing specific HEB expressions and facies tracts.

(A) INTRODUCTION

Bed character and bed stack architecture are two key elements controlling the heterogeneity of deep-water turbidite systems. The former represents the depositional record of sediment gravity flows at a given location with the vertical sequence of grain-size, textures and sedimentary structures recording flow evolution in time and space (Bouma, 1962; Lowe, 1982; Mutti, 1992; Kneller, 1995; Kneller & McCaffrey, 2003). The latter is set by the longer term response of the system to variations in flow volume and concentration over many events modulated by the inherited seafloor topography (Prélat et al., 2010; Brunt et al., 2013b; Marini et al., 2015a). Both define the character and distribution of sedimentary sub-environments in deep-water systems.

A wide range of sediment gravity flow deposits have been recognised in turbidite systems. They include the well-known Bouma-type graded sandstones and muddier and mostly ungraded debris flow deposits (including all transitional members; see Mutti, 1992; Mulder and Alexander, 2001). However many sandstone beds include co-genetic argillaceous and often mudstone-clast rich divisions in their upper portion. These strata are referred as hybrid event beds (HEBs; Haughton et al., 2009), and are recognised as a key element of deep-water systems across a wide range of scales and tectonic settings (Van Vliet, 1978; Mutti et al., 1978; Haughton et al., 2003; 2009; Talling et

al., 2004; 2012; Amy & Talling, 2006; Hodgson, 2009; Muzzi Magalhaes & Tinterri, 2010; Kane & Pontén, 2012; Southern et al., 2015; Fonnesu et al., 2015; 2016; Kane et al., 2017). If present in subsurface hydrocarbon reservoirs they can severely compromise their performance (Amy et al., 2009; Porten et al., 2016). Many mechanisms have been invoked for their formation involving a range of flow behaviours, but they are generally interpreted as deposits formed by down-dip flow transformation from a turbidity current to an increasingly cohesive flow (Haughton et al., 2009). Nevertheless their bed make-up can be very variable particularly in term of the texture and character of the argillaceous sandstone division. The latter can include large mudstone rafts (m-scale) embedded in a relatively clay-poor sandy matrix (Haughton et al., 2010; Fonnesu et al., 2015; 2016; Southern et al., 2015), mudstone-clast rich debrites (Haughton et al., 2003; Talling et al., 2004; Hodgson, 2009; Patacci et al., 2014; Fonnesu et al., 2015; 2016), clast-poor but clay-rich sandstones (Talling et al., 2004; 2012), or beds with mud-rich 'starry-night' texture (sandy mudstones; Lowe & Guy, 2000; Barker et al, 2008; Haughton et al., 2009). Thick and extensively banded beds (*sensu* Lowe & Guy, 2000) are also sometimes found associated (Barker et al., 2008; Davis et al., 2009) or banded divisions can occur directly beneath argillaceous sandstones in composite hybrid event bed types (Haughton et al., 2009; Kane & Pontén, 2012; Tinterri et al., 2016). Despite their very variable character, the occurrence of each HEB types has rarely been linked to its stratigraphic or palaeogeographical position within deep-water depositional systems.

HEBs are commonly found as a major bed motif in unconfined distal and lateral fringes of distributive lobe systems (Haughton et al., 2003; Hodgson, 2009; Kane & Pontén, 2012; Kane et al., 2017; Spychala et al., 2017) where they replace beds composed dominantly of clean sandstone either up-dip or axially (Fig. 1A). They are usually concentrated at the base of prograding lobe packages in vertical 1D successions as fringes to lobe bodies deposited further upslope (Hodgson, 2009; Kane & Pontén, 2012; Kane et al., 2017; Spychala et al., 2017). Their occurrence is interpreted to reflect the progressive deceleration of clay-enriched flows in which the turbulence was suppressed as flow energy dissipated on flatter and more distal fan sectors. A type of matrix-rich sandstone, resembling hybrid event beds, is also recognised in more proximal locations in the

fringes of channel splays (Terlaky & Arnott, 2014). In this case the turbulence suppression is attributed to a combination of fines-entrainment and rapid deceleration of plane-wall jets produced by upslope channel avulsions, as the jets expand into externally unconfined areas. In both cases hybrid event beds are found systematically interbedded with other sandy turbidites in a pattern interpreted to reflect the progradation or lateral switching of depositional sub-environments.

HEBs are also an important element in the aggradation of extensive basin plains (Ricci Lucchi & Valmori, 1980; Amy & Talling, 2006; Muzzi Magalhaes & Tinterri, 2010; Tinterri & Muzzi Magalhaes., 2011; Marini et al., 2015a). In these cases they form thick and sheet-like extensive beds (almost basin-wide) in stacks with poor vertical organisation and an overall aggradational trend (Fig. 1B). Long-distance facies tracts extending 10s km to 100s km for individual event beds have been documented in the laterally-confined basin plain of the Miocene Marnoso Arenacea (NW Italy). Here bed correlations show an overall increase of the matrix-rich sandstone at the expense of underlying matrix-poor sandstone moving distally until beds gradually or abruptly pinch out (Ricci Lucchi & Valmori, 1980; Amy & Talling, 2006; Talling et al., 2012). Hybrid event beds in this setting are interpreted to have been deposited by a spectrum of depositional processes ranging from: 1) debris flows released from upslope and partly transforming to a forerunning turbidity current (Haughton et al., 2003) or late stage basal sand settling from a plug flow (Baas et al., 2009; Sumner et al., 2008; Talling, 2013); 2) erosion of mud-rich seafloor resulting in bulking and generation of a subsidiary debris flow (Mutti et al., 1978; Mutti & Nilsen, 1981; Talling et al., 2004; Amy & Talling, 2006; Haughton et al., 2009; 2010; Fonnesu et al., 2016); 3) generation of a debris flow by rapid deceleration and collapse of a turbidity current (Talling et al., 2004; Haughton et al., 2010).

The present study is drawn from the Cretaceous-Paleocene Gottero turbidite system located in the Ligurian Apennines in NW of Italy (Abbate & Sagri, 1970; Nilsen & Abbate, 1984; Marini, 1991). The spectacular exposures and the wide range of deep-water sub-environments recognised, ranging from proximal channels, unconfined proximal and distal lobes and confined basin plain deposits, as well as the abundance and variability in the types of hybrid event beds, make this an instructive

case study to investigate variable HEB character and distribution through the system. The examples provided highlight how different hybrid event bed types occur preferentially in certain deep-water sub-environments and the possible controls on their deposition. Furthermore the sedimentological analysis of hybrid event beds and their documented lateral transitions gives insight into the mechanisms and the range of flow transformations (and related facies tracts) that occurred in both proximal and distal sectors of the Gottero turbidite system.

(A) GEOLOGICAL AND STRATIGRAPHIC SETTING

The Gottero system is a relatively small deep-water turbidite system of Maastrichtian - Early Palaeocene age (Passerini & Pirini, 1964; Elter et al., 1997; Marroni & Perilli, 1990; Marroni et al., 2004) developed on oceanic crust in a trench basin (Abbate & Sagri, 1970; Nilsen & Abbate, 1984). It was subsequently deformed and thrust north-eastward as an allochthonous sheet in the Eocene and Oligocene during the Alpine-Apennine Orogeny becoming part of the Liguridi structural domain (Marroni et al., 2004). Today the Gottero outcrops extend discontinuously for about 70 km along the eastern Ligurian coast between Genova and Carrara and for about 45 km inland toward the Ligurian Apennines in northwest of Italy (Fig. 2).

The Gottero system developed in a complex Late Cretaceous palaeogeographic setting on the floor of the Ligure Piemontese Sea during the E-W convergence between Europe and Adria plates (see Marroni & Pandolfi, 2007; Marroni et al., 2010). Calcareous turbidites were fed from the Alps to form the Helminthoid flysch sequences (Sholle, 1971; Sagri, 1974) and a series of siliciclastic flysch units referred to as the Gottero, Elba, Novella, Mt. Venere and Bordighera were sourced from the southwest off the Corsica-Sardinian block (Abbate & Sagri, 1982). Sediment dispersed from the two source areas (clastic and carbonate) only rarely mixed as they filled two basins separated by an inferred topographic ridge (the Bracco high; Elter & Raggi, 1965).

The Gottero system belongs to the internal basin sector (Internal Liguridi; Fig. 2) which includes oceanic lithosphere and sedimentary deposits formed within the Ligure-Piemontese Sea between the Jurassic and the Paleocene (Fig. 3) first during extension and then convergence. The basement

is composed of oceanic crust including Jurassic lherzolites, gabbros and pillow lavas (Bortolotti & Passerini, 1970). The overlying sedimentary cover is made up of: Callovian-Santonian basinal deposits comprising the Diaspri radiolarian cherts, Calpionella limestone and Palombini shales (Elter et al., 1997; Marroni, 1991); a thick (c.1100 m thick) Santonian-Maastrichtian succession comprising siliciclastic basin-plain turbidites forming the Lavagna Group; and the Maastrichtian – Early Paleocene (Monechi et al., 1984, Elter et al., 1997) Gottero sandy deep-water turbidite system. The succession is unconformably overlain by the Early Paleocene Giaiette Shales (Passerini & Pierini, 1964) a >300 m thick chaotic unit (interpreted as mass transport complex; MTC) containing blocks of Gottero Sandstone and exotic material in the form of siliceous limestones, cherts and ophiolite blocks (Marroni & Pandolfi, 2001). The whole sequence records the trenchward motion of a portion of the Ligure Piemontese oceanic lithosphere until its involvement in the Eo-Alpine accretionary prism (Marroni et al., 2004). The Gottero system is therefore attributed to an evolving trench basin developed above an eastward-directed subduction zone.

The Gottero sandstones are feldspathic greywackes containing fragments of metamorphic, volcanic and sedimentary rocks (Malesani, 1966; Pandolfi, 1997) derived from the Sardo-Corso massif where large igneous crystalline masses were exposed (Parea, 1965; Valloni & Zuffa, 1981; Van de Kamp and Leake, 1995). Although upper slope or shallow-water equivalents are not preserved, the southern provenance for the Gottero sandstones is consistent with the regional palaeoflow indicators which are mainly directed towards the north and northeast (Fig. 2; Parea, 1965; Nilsen & Abbate, 1984). Limited changes in petrographic composition are recognised laterally across the Gottero outcrop belt and with stratigraphic position (Pandolfi, 1996; 1997) suggesting a relatively stable source area and confirming that the different components of the Gottero likely belong to a single system. An exception is the presence of several beds with an ophiolitic provenance (Pandolfi, 1997) in the uppermost part of the Gottero succession at the Mt. Ramaceto locality (Fig. 3) interpreted to have been sourced from an uplifted accretionary prism which provided sediment to the trench during the last phase of basin filling. The Gottero system crops out in two branches

(the eastern Mt. Ramaceto - Mt. Zatta and the western Mt. Gottero - Mt. Molinatico) separated by the Bracco ophiolite massif (Elter & Raggi, 1965). Sedimentation in the two areas was probably diachronous with siliciclastic sedimentation in the eastern Gottero beginning during the Coniacian-Santonian (Vescovi et al., 2002) whereas in the western part of the system deposition commenced in the Campanian-Maastrichtian (Marroni, 1991).

(B) Stratigraphy of the western Gottero system

The present study focuses on the portion of the Gottero Sandstone cropping out on the western side of the Bracco massif. Data were collected from six locations (Monterosso, Deiva Marina, Moneglia, Terrarossa, Mt. Ramaceto, Mt. Zatta; Fig. 3), five of which are aligned along a SE-NW transect roughly parallel to the general palaeoflow direction (Fig. 4). The lack of continuous exposure precludes direct correlation of individual stratigraphic elements but the enclosing stratigraphic units and the main internal lithostratigraphic boundaries and trends can be consistently recognised across the area. The earliest of the sandstone bodies comprise four sand-rich units interfingering with fine-grained deposits of the Lavagna Group in the north-western sector of the basin which are defined as the “Lower Gottero” (Casnedi, 1982; Marini, 1991). They are interpreted as channelized bodies and lobes of an early prograding and unconfined fan system. The overlying “Upper Gottero” was deposited above a widespread 20 to 40 m thick mud-rich chaotic deposit (Vallai MTD). The upper Gottero succession begins with a fine-grained slope and basin plain wedge (Gottero 1; GOT1) followed by coarse-grained sand-rich basin floor succession (Gottero 2; GOT2) extending from the proximal Monterosso section to the more distal sections on Mt. Ramaceto and Mt. Zatta without important facies or thickness changes (Fonnesu, 2016). The boundary between the underlying fine-grained units and the Gottero 2 sandstones is sharp and erosive in the Monterosso locality, but it appears transitional at Moneglia, Mt. Ramaceto and Mt. Zatta where the same contact is recorded by an obvious thickening-upward trend. The overlying unit (Gottero 3; GOT3) shows an overall backstepping trend expressed in both proximal and distal locations. An unconfined turbidite fan developed in more proximal areas (Monterosso, Moneglia) but in the distal areas (Mt. Ramaceto and Mt. Zatta) tectonic activity created basin segmentation.

The Gottero system thus developed two separate distal depocenters in the Mt. Ramaceto and Mt. Zatta areas where 825 m and 640 m of Gottero 3 succession accumulated, respectively, separated by a tectonic high (Marini, 1991; 1994). The two areas evolved separately, with the Mt. Zatta succession dominated by stacked outer-fan lobe packages together with an interbedded local MTD, whereas the Mt. Ramaceto depocentre developed into a confined basin plain (*sensu* Mutti & Johns, 1978; Remacha et al., 2005; Mutti et al., 2009; Pickering & Hiscott, 2015; Fonnesu et al., 2015) in which very thick, tabular and laterally-extensive event beds with thick mudstone caps are interbedded with thin-bedded packages (Fonnesu et al., 2016). The down-dip basin margin responsible for late basin confinement is not preserved in the outcrop but it could be represented by the Bracco palaeo-high (Fig. 2).

The overall stratigraphic trend recorded by the Gottero can be interpreted as comprising a first phase in which the system developed as an unconfined and radial-shaped basin floor fan with the basin boundaries outside of the actual outcrop area. With narrowing of the trench due to syn-sedimentary uplift of the Alpine accretionary prism, local subsidence and progressive confinement of the distal sectors of the basin occurred, but the proximal fan area would still have remained relatively unconfined (Nilsen & Abbate, 1984; Fonnesu, 2016). The presence at Gottero 3 time of separate distal basin depocenters that cannot be easily correlated (Marini, 1991; 1994) might reflect active segmentation of the trench basin during development of the accretionary prism (Fonnesu, 2016) until it finally collapsed into the trench causing the regional erosive unconformity at the base of the chaotic deposits of Giaiette MTC unit (Fig. 4).

(A) DATASET AND METHODOLOGY

About 5200 metres of sedimentary logs have been collected from the six outcrop localities (Figs 3 and 4), 4307 metres of which were measured bed-by-bed at 1 cm resolution mainly using a Jacob's staff (e.g. a 1.5 metre high rod equipped with a clinometer and a flat sighting disc). The remaining ca. 800 metres of logs were drawn by using photomosaics of inaccessible cliff sections. Because most of the coastal sections crop-out on vertical cliffs and the bedding is often vertical or steeply

dipping, the lateral exposure is no more than 50 meters in most cases. An exception is the area around Monterosso, where beds can be traced on vertical cliffs laterally for about 400 metres. The Gottero Sandstone Formation can be mapped from Moneglia to Mt. Ramaceto as a continuous body on the limbs of a regional syncline with the Giaiette Shales at its core (Marini, 1991; Marroni et al., 2004) (Fig. 3). Nevertheless the exposure is very poor between these two localities, with the exception of an abandoned quarry located in Terrarossa where about 140 metres of Gottero Sandstones crop out. The most spectacular exposures of the Gottero system are located on Mt. Ramaceto (Casnedi, 1982; Marini, 1994; Fonnesu et al., 2015; 2016) where the entire succession can be logged over a total thickness of 1075 m (Fig. 5). The uppermost 735 m of the Gottero can be traced for about 4 kilometres in a N-S direction and bed-by-bed correlations were established between eight measured stratigraphic logs. The succession at Mt. Ramaceto is overturned (apart from the southernmost section) being mostly on the inverted limb of a regional syncline (Casnedi, 1982; Marroni, 1991; Marroni et al., 2004). The Mt. Zatta Gottero succession is 810 m thick and located slightly off-axis with respect to the cross-section shown in Fig. 4. Samples were collected from specific hybrid event beds and their internal texture has been analysed with optical microscopy (13 thin-sections). Clay content and framework mineralogy has been quantified petrographically by point counting (500 points per section).

(A) BED TYPES AND HYBRID EVENT BED CHARACTER

The Gottero system includes a wide range of gravity flow deposits ranging from large mass-transport deposits, debrites, high and low-density turbidites, limestone beds through to a large variety of hybrid event beds. The wide range in grain-size available in the system (Nilsen & Abbate, 1984), ranging from boulders to very fine sand and silt, means that there is a wide variety of facies types in deposits belonging to different sub-environments. Five bed type groups are distinguished: debrites, DEBs; gravelly high-density turbidites, GHDTs; high-density turbidites; HDTs; mudstone-clast rich beds, MRBs; low-density turbidites, LDTs; limestone beds, L; and hybrid event beds, HEBs) (Tab. 1). This paper focuses on the character of the hybrid event beds (HEBs), which are therefore described in more detail. Because the entrainment of mud clasts is

considered an important process in their formation, an additional bed type class termed "mudstone clast rich beds" (MRBs) is also defined to include high-density turbidites carrying abundant mudstone clasts usually clustered in the uppermost structureless bed portion (see Mutti & Nilsen, 1981; Postma et al., 1988; Fonnesu et al., 2015). Unlike some types of hybrid event beds, mudstone clasts in MRBs are generally less densely packed and are dispersed in a clean sandstone instead of a clay-enriched sandstone. In the distal confined part of the system, mudstone clast-rich beds show tabular geometries and are found in close spatial association with mudstone clast-rich hybrid event beds (Fonnesu et al., 2015). Therefore they are likely to represent deposits of flows during the early stages of hybrid flow development.

(B) Hybrid event beds (HEBs)

Hybrid event beds are characterised by a vertical association of a basal clean (interstitial-clay poor) and mostly structureless sandstone (termed H1 by Haughton et al., 2009) and argillaceous sandstone (commonly with a swirled fabric or chaotic appearance) in which there are variable concentrations of mudstone clasts and sheared sand patches (H3). Other divisions can also be found but are not always present (Haughton et al., 2010; Talling, 2013) such as: an interval with scattered mudstone clasts at the transition between the clean and argillaceous sandstone (H1b); an interval comprising alternating paler and darker sandstone bands (H2); a fine/very fine grained parallel to ripple laminated division deposited on top of the argillaceous sandstone (H4); and a silty mudstone cap (H5). These facies are never observed in an inverse or different order. Because the H1 division tends to be thin and pinch out in distal and lateral locations (Haughton et al., 2003; Amy & Talling, 2006) it is possible that some hybrid event beds are expressed just as argillaceous sandstone facies (H3) (Davis et al., 2009) capped by a fine-grained structured sandstone (H4). Hybrid event beds are here classified mainly on the basis of the texture of the H3 division and of the size and shape of the clasts within it. H3 divisions show a range in terms of the intensity of soft-sediment deformation, ranging from intact substrate blocks to a well-mixed argillaceous sand, passing through deformed slump-like and mudstone clast-rich textures from which specific sub-facies are distinguished (Fig. 6). Other characters such as bed thickness, presence of H2 or H4

divisions and type of sole structures are used as complementary criteria (Tab. 2). The H3 facies types form a continuum from which six representative bed types have been identified varying from HEB-1 to HEB-6 (Fig. 6). Bed type classification refers to the aspect of a bed in one location but individual beds can change from one type to another over a relatively short distance (Hodgson, 2009; Fonnesu et al., 2015) along lateral or longitudinal facies tracts (see Mutti, 1992; Mutti et al., 2003).

(C) HEB-1

HEB-1 are very thick tripartite event beds (0.60 - 6.80 m thick; average 3.32 m) characterised by the presence of large and relatively undeformed substrate rafts (bedding-parallel, elongated slabs with long axes much greater than the bed thickness; 0.5 - 2 m thick and up to 20 m long). The rafts are supported by a poorly-sorted, coarse- to fine-grained sandstone matrix including mudstone chips, mud-poor sand patches and sand injections. Substrate rafts can be dark mudstone (RI) or bed-parallel or gently dipping thin-bedded sandstone-mudstone units in some cases with thin limestone beds (SP) (Fig. 6). Lateral bed correlations highlight that the base of these beds is often erosive; producing 1 to 2 m deep and 100s of metres wide scour features. The type of raft contained in the H3 division can often be matched to the substrate encountered directly beneath the event bed when it is traced laterally to less deeply eroded sectors. Thus the presence of rafts comprising mudstones with thin-bedded sandstone is typical of event beds that overlie similar *in-situ* thin-bedded sections, whereas mudstone rafts are usually found in HEBs that overlie thick mudstone caps of earlier event beds (Fonnesu et al., 2016). Substrate rafts usually accumulate at the base of the H3 division with their longer axes aligned mostly parallel to bedding. Their upper and lower margins have generally sharp contacts with the surrounding sand-rich matrix or the underlying sandstone but their lateral edges can sometimes be deformed, frayed or preserved breaking into discrete smaller mudstone clasts. The underlying H1 basal division is a very-coarse to medium grained apparently structureless (or very crudely laminated) but generally graded sandstone. The contact between the lower H1 sandstone and H3 is mostly irregular but sharp with the larger rafts often showing evidence of having ploughed into and thinned the basal sandstone or

even occurring fully encased in it suggesting they foundered into what was soft wet sand (Fonnesu et al., 2015). Next to the larger rafts, sand injections extruding from the H1 sandstone division can form large columnar pillars (about 1- 1.5 m in diameter) terminating in *mushroom-like* sill features preferentially developed at the boundary between the H3 and H4 divisions (see Knaust et al., 2014). Slightly deformed, thinner, vertical or inclined sand injections (10-20 cm in diameter) can cross-cut the rafts and the sandy matrix of the H3 division but do not cross the boundary between the H3 and H4 divisions. The effects of dewatering processes are also evident in the texture of the H1 sandstone with sub-vertical but curved dewatering sheets preferentially observed when the top to H1 is dome-shaped or is locally depressed. The H4 division and the H5 mudstone cap are usually well-developed. H4 is present in 94% of HEB-1 beds and is characterised by a fine-grained laminated and/or rippled sandstone division (typically about 35 cm thick) with a very irregular base and flat top. Loading structures with a m-scale wavelength and fine-grained sandstone *ball and pillow* structures derived from the H4 unit are commonly observed foundering into the H3 muddier division, especially where the mud content in H3 is higher (Patacci et al., 2014; Fonnesu et al., 2015; Tinterri et al., 2016). The beds cropping out in the upper part of Mt. Ramaceto succession can also contain unusually thick H4 divisions including repetitions of structureless and laminated intervals, H5 intervals composed of a silty homogenous facies and a very thick mudstone cap (sometimes above 3 m thick). The same character is shared by other HEB types (HEB-1 to 4) present in the same stratigraphic interval.

(C) HEB-2

HEB-2 beds are very thick, tripartite event beds (0.40 - 9.57 m thick; average 2.37 m) characterised by a heterogeneous and chaotic H3 division. This is made up of folded pieces of thin-bedded stratigraphy (SC) or by a complex sand-injection network (MCI) set in a mud-rich matrix (Fig. 6). Both facies can be interpreted as an advanced deformation stage of heterolithic or mudstone slabs respectively (Fonnesu et al., 2016). Despite their chaotic appearance, these beds can be distinguished from gravitational slump deposits because they are consistently associated with a thick sandy base (H1) and a laminated graded sandy top (H4), and because they pass laterally into

other hybrid bed types. The H3 divisions in these beds are characterised by abundant well-developed soft-sediment deformation features such as: 1) intense folding of thin-bedded packages deformed into complex isoclinal and/or recumbent folds; 2) dismembering of sand levels with development of pinch-and-swell structures, attached or detached pseudonodules, ductile shear zones and intense thinning of fold limbs; 3) Deformed sand injections made of coarse-grained and poorly sorted sandstone extruded from the underlying sandy base and bordering or cross-cutting the deformed heterolithic clasts. The deformed strata and the sand-injections are encased in a mud-rich matrix in part produced by squeezed mud-rich blocks. Some of the mudstone appears to be composed of relatively undeformed blocks. However, in other instances the mudstone appears to have behaved in a more plastic way and it seems to be associated with folding having being injected by sand along fold axial planes or sheared out along fold limbs. In other cases, the mudstone can be well mixed with the sand, resulting in a dirty-looking sandstone rich in mm- and cm-sized mudstone clasts. As for HEB-1, the basal H1 sandstone is a structureless, weakly-graded sandstone containing abundant dewatering features and is characterised by an abrupt transition to a muddier H3 division. Also like HEB-1, HEB-2 beds usually (79% of beds) have a well-developed (typically about 35 cm thick) laminated and graded H4 division, loading and sometimes foundering into the underlying mud-rich H3 division.

(C) HEB-3

HEB-3 are generally thick (0.30 - 5.30 m thick, 1.77 m average) hybrid event beds in which the H3 division is composed of densely packed mudstone clasts (MCB; clasts average above 5 cm across) surrounded by a dirty sandstone rich in mm- and cm-sized mudstone clasts (Figs. 6 and 7), clean sandy patches and sand injections. Individual mudstone clasts are rounded to sub-rounded, and have a generally oblate shape aligned parallel to bedding. Mudstone clasts can be randomly distributed, but more often they display a weak normal grading. Clasts are often in contact or separated only by thin veneers of poorly-sorted dirty sandstone. The inter-clast sandstone has a ratio of interstitial clay vs. clast framework varying from 15 to 21%, showing generally a progressive higher quantity of detrital pore-filling clay and mica flakes towards the upper part of

the division (Talling et al., 2004; Hodgson, 2009). The value seems to increase in parallel with the concentration and disruption of the mudstone clasts. The H3 division can be laterally continuous or form lenses in which the clasts are more densely packed separated by portions in which clasts are less common and surrounded by cleaner sandstone (Patacci et al., 2014; Fonnesu et al., 2015). The latter facies can also form a transitional unit between the basal H1 sandstone and the H3 division (H1b). The relative proportion of H1 and H3 divisions can be highly variable, with event beds ranging from being H1-dominated to H3-dominated without important changes in the H3 texture over short length scales (10s to 100s m). Bed bases are often extensively grooved and can be characterised by widespread but cryptic composite and multiphase erosional features comprising elongated shallow scours (a few metres long and a few tens of cm deep) associated with lateral sand injections and rip-up clasts from the underlying substrate (Fonnesu et al., 2016). An uppermost H4 division is developed in most cases (87%) and typically is about 25 cm thick; it commonly has tabular boundaries, but local metre-scale wavelength load casts can also occur. HEB-3 represents the most common type of hybrid event bed in the logged Gottero system (Tab. 2).

(C) HEB-4

HEB-4 are thick to mid-size beds (0.20 - 3.20 m thick; 0.92 m average) comprising an H3 division with abundant cm-size mudstone clasts (typically about 2-5 cm across) set in a dirty (21 to 23% dispersed clay), medium to fine-grained sandstone matrix (MCD) (Fig. 6). Mudstone clasts, despite being of smaller size than in HEB-3 beds, are still abundant and display many clast-to-clast contacts. As in HEB-3, mudstone clasts are usually disc-shaped, can be randomly orientated or be sub-parallel to bedding and can show a weak normal grading. Similarly, the matrix of the H3 division can display a subtle upward increase in the mud content. The contact between the H3 division and the basal H1 sandstone is usually sharp but undulose with m-scale wavelength and 10-30 cm amplitude irregularities (Fonnesu et al., 2015). An H4 division is commonly present (82%) but is usually thin (typically about 15 cm), normally graded and planar laminated.

(C) HEB-5

HEB-5 are event beds ranging from 0.05 to 2.40 m in thickness (average 0.44 m) with the H3 division constituted by well-mixed argillaceous sandstone with scattered mudstone clasts (MDC) (Fig. 6). The matrix is enriched in clay (25-27 %) as well as hydraulically 'light' components such as mica flakes, clay flocs and organic matter, which generally tend to concentrate toward the top of the H3 division (Fig. 7). The contact between the H1 and H3 divisions is sharp in the majority of the cases but in a few beds, an intervening banded H2 division is developed in the form of dark clay-prone sandy layers alternating with lighter fine-grained cleaner sandy intervals (Lowe and Guy, 2000; Haughton et al., 2009; Davis et al., 2009). H1 is a poorly to well-sorted and weakly graded, coarse to medium grained sandstone. The bed base is generally sharp, decorated with both grooves and flutes, the latter generally absent in the other hybrid event bed types. In a few cases HEB-5 beds do not have a basal H1 sandstone and the H3 division dominates the event bed. The H4 division is not systematically developed (occurring in only 48% of beds). Nevertheless, whenever H4 is present, it forms a thin planar or ripple-laminated unit capping the bed that commonly loads and founders into the H3 argillaceous sand below, with an associated development of pseudonodules.

(C) HEB-6

HEB-6 are a relatively uncommon type of hybrid event bed. They have an average thickness of only 0.2 m (0.12 to 0.75 m) and are distinguished from all the other hybrid bed types in that the basal division is a fine-grained parallel or ripple laminated sandstone overlain by a weakly graded fine-sandstone to clay-enriched fine-grained sandstone (MD) (Fig. 6). The bed has an upward transition directly to a dark capping mudstone.

(C) Hybrid event bed morphometrics

Although the Gottero hybrid event beds can be assigned to one of six types guided mainly by the character of their H3 divisions, data show a clear correlation between HEB type and their average and maximum thickness (Tab. 2; Fig. 8A). It can be observed that beds from HEB-1 to HEB-6 follow a thinning trend, with HEB-5 and HEB-6 being much thinner than the other types. On the

other hand, a clear relationship between the ratio of H1 to H3 thicknesses and HEB type is not observed (Fig. 8B). HEB-3 seems to have a higher variability of H1/H3 ratio, with a larger number of beds with relative thin H1 divisions. HEB-5 beds more commonly lack an H1 division.

(C) Interpretation

The variability in the hybrid event character observed in the Gottero system and captured by the six-fold classification scheme is comparable with the bed model described by Haughton et al., (2009). The hybrid event beds described above are interpreted as the deposits left by the passage of individual flows, the rheology of which evolved from being poorly cohesive and essentially turbulent to being more cohesive and turbulence-suppressed (Haughton et al., 2009). As discussed below, the range of bed types is thought to reflect the variable manner of mud entrainment, the way in which the flow was partitioned rheologically, and the mechanism of turbulence damping. (Baas et al., 2009; 2011; Patacci et al., 2014; Fonnesu et al., 2015; 2016).

The basal structureless or weakly stratified H1 sandstone is interpreted as deposited by a sandy high-concentration turbidity current (Haughton et al., 2003; 2009). Deposition was probably characterised by a high-rate of sediment fallout, causing the intense dewatering observed in most H1 divisions and the sand-injections into the overlying H3 division; the sandy basal divisions were prone to liquefaction when dynamically loaded by the H3 divisions. The normal or coarse-tail grading and the occasional presence of traction structures suggest that there were also phases during which layer-by-layer deposition under traction and hindered settling from a non-cohesive flow dominated (Kneller & Branney, 1995). The argillaceous sandstone divisions (H3) with their variety of chaotic or weakly-organised mudstone and heterolithic clasts, show evidence of *en-masse* deposition. Deposition of the H3 clay-enriched sandstones is interpreted to be related to three main processes: 1) Rapid entrainment of large quantities of mud-rich substrate material which became partially disaggregated in a shearing near-bed layer (Haughton et al., 2009; Fonnesu et al., 2015; 2016). 2) Vertical top-down transformation from turbidity current to debris flow due to rapid flow deceleration (Sumner et al., 2009; Baas et al., 2009; Kane & Pontén, 2012). 3) Longitudinal transformation due to lateral hydrodynamic fractionation of clay and flaky particles

(Haughton et al., 2009; Pyles et al., 2013). The first process is thought to be responsible for formation of HEB-1 to HEB-4 beds. The second and the third processes are interpreted to have operated in the case of HEB-5 and HEB-6 beds.

A rheology change between the turbulent flow responsible for the deposition of the basal sandstone (H1), and the mostly cohesive laminar flow depositing the H3 division, can be inferred from the presence of progressively more abundant mudstone clasts vertically in the bed (including the development of H1b). The clasts might have been kept in suspension in the upper and rearward part of the dense flow due to their low density and resulting buoyancy (Mutti & Nilsen, 1981; Postma et al., 1988). Alternatively, and less commonly, the flows oscillated between a frictional and a laminar condition, leading to the formation of a banded interval (H2 – Lowe & Guy, 2000; Haughton et al., 2009; Baas et al., 2011). The common presence of an overlying graded and laminated H4 division grading into a mudstone cap (H5) suggests the re-establishment of turbulent flow conditions from a trailing wake followed by sediment fallout from the suspension cloud. The geometry of the H4 division may reflect the rheology of the just-deposited underlying H3 division (Fonnesu et al., 2015; Tinterri et al., 2016). Loaded or foundered H4 divisions might be produced by the wakes to flows decelerating on a very heterogeneous, plastic and mud-rich H3 deposit; a planar boundary suggests a more homogenous and semi-rigid behaviour.

(A) FACIES ASSOCIATIONS AND SUB-ENVIRONMENTS

Hybrid event beds and other sediment gravity flow deposits are diversely stacked throughout the Gottero system but can be grouped in specific facies associations. Following the approach of Mutti and Ricci Lucchi (1972) (see also Mutti & Normark, 1987; 1991), each facies association can be considered the stratigraphic expression of a specific sub-environment within a turbidite system, interpretation of which is tied to its characteristic bed stack, general architecture and stratigraphic/palaeogeographic position. Five sandy facies associations and have been identified in the Upper Gottero system (Fig. 9): FA-A) inner fan channels; FA-B) mid-fan lobes; FA-C) outer-fan lobes; FA-D) weakly amalgamated sheets; and FA-E) isolated basin plain sheets. An additional

facies association (FA-F) includes the remaining dominantly fine-grained facies comprising slope deposits and fine-grained basin plain facies. Facies association terminology has been partially retained from a previous and prescient sub-environment fan zonation for the Gottero system proposed by Nilsen & Abbate (1984). The proximal Gottero area is dominated by FA-A to FA-C facies associations (Monterosso, Deiva Marina, Moneglia, Terrarossa), representing deposits of a relatively unconfined fan system. The external part of the system (Mt. Ramaceto) is characterised by facies associations FA-D and FA-E and is interpreted as a confined basin-plain environment. The Mt. Zatta succession includes interleaved facies associations of both types in a separate overfilled trough (Marini, 1995). Quantitative log data allow a reliable estimation of characteristic sedimentological parameters such as overall sandstone percentage (St%; includes locally conglomeratic basal divisions of event beds, and clayey sandstone forming H3 divisions in HEBs), component bed types and in particular the abundance and types of hybrid event bed present in each of the facies associations. However, the dimension of large- and medium-scale depositional features such as channels and lobes, and the establishment of their internal hierarchy can only be achieved in a limited number of cases due to the rarity of laterally continuous exposures.

(B) FA-A Inner fan

The most proximal preserved section of the Gottero system is dominated by conglomeratic and coarse-grained sandy deposits in which the sandstone percentage is extremely high, reaching 99% (Fig. 9A). The only outcrop example of this facies association is located in the Monterosso area (Nilsen & Abbate, 1984; Pandolfi, 1996). The succession includes: an erosive coarse-grained lenticular unit (25 m thick at the axis), interpreted as a channel-body; and a thicker and generally more tabular sandbody, of minimum 250 m thickness (the top cannot be constrained because it has been removed by modern marine erosion). Dominant facies includes mudstone-clast conglomerates, clast-supported lags, and amalgamated coarse-grained turbidites including traction carpets, mudstone clasts and large scale cross-beddings. Shallow erosive “cut-and fill” features (Mutti & Normark, 1987), uneven bed bases (local erosional relief up to 1.5 m), grain-size breaks, and rapid lateral bed thickness changes, determine important bypass occurring in the area. The

facies association is interpreted to represent a proximal fan environment spanning base-of-slope channels to channel-month (channel-lobe transition) settings. Despite the common presence of substrate erosion and rip-up clasts, hybrid event beds are not present in this facies association in either the channelized or the more tabular units (Fig. 9A).

(B) FA-B Mid-fan lobes

The intermediate part of the Gottero system and most of the Gottero 2 unit (Deiva Marina, Moneglia, Terrarossa, Mt. Ramaceto, Mt. Zatta sections; Fig. 4) are composed of mainly parallel-bedded, amalgamated strata forming 10 to 20 metres-thick sandstone packages organized in thinning- and fining-upward sequences (Fig. 10A-B). These sequences are separated by thinner (metres-thick) mud-prone intervals sometimes containing thin-bedded sandstones. This forms a facies association with an overall St% of 88% (Fig. 9B).

The base of individual sandstone packages is alternatively sharp or scoured into the thin-bedded unit underneath (Fig. 10C). Sandstone packages are made up mostly of ungraded and poorly sorted very coarse (occasionally granule grade) to coarse grained sandstone beds (Fig. 10D), rich in dispersed and often angular mudstone clasts some of which are armoured (Fig. 10E). Tractive granule layers and clast-supported conglomeratic lenses directly overlain by horizontally laminated and rippled fine-grained sandstones facies are common (Fig. 10F), showing evidence of flow bypass. These bodies are interpreted as relatively proximal mid-fan lobes (see Mutti & Ricci Lucchi, 1972; Mutti & Normark, 1987). The top of each of the lobes is marked by an abrupt change to a relatively thin (about 1-2 m thick) mud-prone unit constituted by thin-bedded events. These finer-grained intercalations are laterally continuous and are consequently interpreted as inter-lobe deposits and related to phases of reduction in sediment supply to the basin.

Hybrid event beds are present as rare thin clast-poor hybrid event beds (generally HEB-5; Fig. 10G) interbedded with thin bedded turbidites, siltstone and mudstone in the inter-lobe deposits. In few cases thick and clast-rich or raft-bearing types (HEB-3; more rarely HEB-2 and HEB-1) as the first bed at the base of the lobe packages. These beds systematically overlie a mud-rich inter-lobe

package and in a few cases show evidence of partial detachment of the underlying substrate by lateral injection from the base of the bed. Besides these occasional HEBs, a distinctive hybrid-rich interval is found at the base of Gottero 2 unit marking the stratigraphic initiation of the fan. Hybrid event beds in total represent only 8% by thickness of the facies association (Fig. 9B).

(B) FA-C Outer-fan lobes

The intermediate part of the system in the Gottero 3 unit (in Moneglia and Terrarossa localities; Fig. 4) is dominated by 5-20 m thick, thickening-upward or symmetric bed sequences (Fig. 11) constituted by coarse-grained and poorly sorted high-density turbidites, mudstone clast-rich beds and hybrid event beds (Fig. 12). These are interbedded with heterolithic sandstone-mudstone packages containing thin-bedded LDTs and HEBs. The overall St% is estimated at 79% (Fig. 9C). The basal boundary of the sandy packages with inter-bedded fine-grained units is characterised by a progressive upward coarsening and thickening of the beds. The upper boundary can be sharp and marked by a bypass surface or expressed by a more progressive bed thinning. Beds constituting the sandy packages exhibit lateral continuity (but rapid thickness changes) at 100s m outcrop-scale, but are poorly correlated at km-scale. The high-density turbidites generally have very thin mudstone caps (average sandstone-to-mud cap ratio about 3:1) and in most cases they comprise only a basal sandstone, with no laminated upper division. Many beds have angular to sub-rounded mudstone clasts (sometimes armoured) mostly concentrated at the very top of the bed (MRBs: 36%). Conglomeratic lenses or beds including granule traction carpets are also occasionally present.

These characteristics define a sub-environment where turbidity flows bypassed their finer grain sizes which are mostly missing and were presumably transported further down-dip. The sandy units are interpreted as relatively distal outer-fan sandstone lobes. The complex changes in the vertical bed thickness stacking are interpreted as an effect of local lobe progradation (Mutti & Ghibaudo, 1972; Mutti & Ricci Lucchi, 1972), compensational stacking (Mutti & Sonnino, 1981) or autocyclic lateral lobe axis switching (Macdonald et al., 2011; Prélat & Hodgson, 2013). Lateral lobe switching is also suggested by the repeated deviations in the palaeoflow indicators (from WNW to ENE) in the Moneglia locality where this facies association is prevalent (see Fig. 3).

Thin-bedded mud-prone packages are interpreted as distal or lateral lobe fringes rather than allocyclic phases of reduced sediment supply, because of their poor correlatability between lateral sections.

Hybrid event beds represent 15% by thickness of this facies association (Figs. 9C, 12). The most common HEB types include HEB-5 (49% of all HEBs) and HEB-6 (13% of all HEBs). Hybrid event beds with larger mudstone clasts (HEB-3 and HEB-4), substrate slabs (no larger than 2 m) and chaotic textures (HEB-1 and HEB-2) are rare and usually found as outsized event beds directly overlying a mudstone-rich package. HEB-5 and HEB-6 beds are mostly found at the base of thickening-upward lobe cycles together with mudstone-clast rich beds of similar size or as part of thin-bedded inter-lobe packages. They can be vertically organised with beds having relatively thinner H1 divisions located at the base of the thickening-upward cycles and progressively substituted by beds with a thicker H1 division towards the top. Occasionally some thin hybrid beds lack an H1 division, testifying to their very distal position with respect to the axis of the lobe (distal lobe fringe). The HEBs interbedded inside the lobe packages are interpreted as genetically related to the lobe axis cleaner beds and representing the deposits of lateral or frontal lobe fringes (Haughton et al., 2003; Hodgson, 2009; Kane & Pontén, 2012; Kane et al., 2017).

(B) FA-D Basin plain weakly amalgamated sheets

This facies association is constituted by distinctive weakly amalgamated sandy packages (7 to 20 m thick) made of generally thick event beds (mostly hybrid event beds) interbedded with the otherwise poorly amalgamated succession of the Gottero 3 unit in the Mt. Ramaceto (Figs. 13 and 14) and in part of the Mt. Zatta succession. The facies association has an overall St% of about 71% (Fig. 9D). The sandy packages do not display significant lateral thickness variations, at least at scales of up to up to 3 km, but individual beds are poorly correlated due to a high-aspect ratio lenticular shape or display important thickness changes at 100s of m-scale interpreted as compensational patterns (Mutti & Sonnino, 1981) in contrast to the surrounding tabular succession (see FA-E). Beds are coarse to fine grained, well-graded and generally thick, usually preserving a laminated upper division and a thin mudstone cap.

The described units are interpreted as basin plain composite sand-bodies developed in the distal part of the Gottero system (Mutti & Ricci Lucchi, 1972; Mutti & Normark, 1987). The relationships with the more proximal mid-fan and outer-fan lobes are unclear, but they presumably represent separate sand-bodies developed in a down-dip depocentre and are not the distal expression of outer-fan lobes. These units are stratigraphically interbedded and probably genetically associated with the distal Gottero basin plain sheets (FA-F) of which they could represent an architectural pattern developed when the basin was not fully ponded and individual flows could not spread across the entire basin floor developing an internal compensational geometry.

Hybrid event beds are the most common bed type in FA-D units (54% in thickness; Fig. 9D) and include a wide variety of types (HEB-3, 30%; HEB-4 28%, HEB-2, 22%, HEB-1 17%; HEB-5 3%) with the majority on the mudstone clast and raft-bearing types.

(B) FA-E Confined basin plain isolated sheets

The distal sector of the Gottero 3 unit (Mt. Ramaceto and part of Mt. Zatta) is dominated by laterally-extensive, thick event beds (i.e. sheets; Fig. 13) associated with thick mudstone caps, thin-bedded sandy packages and rare limestone and marly intervals (Figs 9E, 15 and 16). The succession has a St% of about 54% on average, and decreasing from the bottom to the top. Grain size of the sandstones varies from very coarse to very fine-grained and beds are generally well graded, without displaying abrupt internal grain size changes or evidence of amalgamation. Many turbidites and hybrid event beds have complex and thick topmost fine-grained divisions including repetitions of structured and unstructured sandstones, wavy sinusoidal laminations and homogeneous silty graded caps with pseudonodules. Those characteristics, in association with thick mudstone caps (average sandstone-to-mud cap ratio for single bed about 1:3), are interpreted to represent the effect of deflection or ponding of the dilute part of turbidity currents (Pickering & Hiscott, 1985; Remacha et al., 2005; Haughton, 2001; Muzzi Magalhaes & Tinterri, 2010; Tinterri, 2011; Patacci et al., 2015). Therefore the present facies association is interpreted as the distal

depositional fill of a confined and relatively sand-rich basin plain (Mutti & Johns, 1982; Remacha et al., 2005; Mutti et al., 2009; Pickering & Hiscott, 2015).

Hybrid event beds in this setting represent the vast majority of the thicker event beds and comprise 31% by thickness of the succession (Fig. 9E). The majority of hybrid event beds are represented by HEB-3 (49%), with the remaining part roughly equally split between HEB-4 (19%), HEB-1 (15%) and HEB-2 (13%). The mixed fine-grained HEBs are very rare with only 5% represented by HEB-5 and no HEB-6. Transitions between different HEBs bed types and between HEBs and MRBs or HDTs are very common along correlative beds. The lateral changes typically involve variations in the proportion of the cleaner basal sandstone and the overlying H3 mudstone-clast rich sandstone divisions and the texture of H3 division. These changes normally occur without substantial variations in the overall bed thickness (Fonnesu et al., 2015).

Hybrid event beds (or more rarely mudstone-clast rich beds) commonly have a scoured base demonstrating the flows were able to erode the underlying substrate for 10s of cm to a maximum depth of about 2 m. Shallow and elongated scours are preferentially found underneath HEB-3 or MRBs. Deeper scour features can be detected from detailed bed-by-bed correlations mostly underneath HEB-1 or HEB-2 beds eroding into earlier mud caps or thin-bedded heterolithic packages.

(B) FA-F Thin-bedded basin plain and slope deposits

Fine-grained thin-bedded intervals are commonplace throughout the Gottero system but only rarely constitute thick (10s to 100s of metres) distinctive packages. These fine-grained and mud-rich units have an average St% of 51%. A widespread and wedge-like fine-grained unit is located at the base of Gottero succession (Fig. 4), making up the Gottero 1 unit (see Marini, 1991). This includes slope deposits with common multi-bed slumps in the proximal Monterosso location to a monotonous succession of thin-bedded, graded and ripple-structured low-density turbidites (LDTs) and occasionally limestone beds (L) in intermediate (Riva Trigoso) and distal locations (Mt. Zatta - Mt. Ramaceto) interpreted as basin plain deposits.

(A) HYBRID EVENT BED GROUPS AND FACIES TRACTS

The sedimentological character of the hybrid event beds, the vertical and lateral bed type changes and transitions, and the facies associations in which they occur, confirm that these beds can have a variable make-up and hence different lateral and longitudinal facies tract expression. The hybrid event bed types described here can be split in two main groups which are thought to have a different origin: 1) beds in which the major component of the H3 division is made up of substrate clasts (ranging from few cm to several metres and 2) beds which include a H3 division with a clay-rich and relative clast-poor texture.

(B) Mudstone-clast and raft-bearing hybrid event beds (HEBs 1-4)

Hybrid event beds attributed to the first class are represented by HEB-1 to HEB-4 types. Beds of these types are mostly found in the confined basin plain areas (FA-D and FA-E) but also (with lower relative abundances) at the base of lobe sequences in more proximal fan areas (FA-B and FA-C), in particularly when the lobe units lie directly on top of inter-lobe fine-grained intervals.

As demonstrated by the physical correlations of the stratigraphically upper part of the Mt. Ramaceto section (Figs. 13 and 16) hybrid event bed types HEB-1 to HEB-4 can be laterally correlated with one another and therefore represent the expression of the same facies tract. A facies tract represents the lateral or longitudinal bed expression of the same depositional event (Mutti, 1992). However, the limited down-dip window in which individual beds can be followed (4 km) cannot capture the complete set of flow transformations in a single correlated bed and multiple beds have to be taken into account in order to reveal the wider t set of lateral transitions. Individual beds show a general down-dip change from thick clean sandstone beds (HDTs) to mudstone-clast enriched hybrid event beds (HEB-1 to 4) (Fig. 17). Field observations suggests that this transition can happen along two distinct facies tract types characterised by different proximal bed types, but with a similar distal expression.

(C) FTH-1 Hybrid flow evolution via entrainment of abundant mud clasts

In the first facies tract type (FTH-1; Fig. 18A), clean HDTs undergo a down-dip change to hybrid event beds by the acquisition, segregation and breakup of cm- to dm-size mudstone clasts. Clasts are thought to have been collected by delamination of relatively local substrate, as demonstrated by the common formation of composite shallow scours (some 10s of cm deep) on the lower surface of the bed (see Bed 14 - Fonnesu et al., 2016). Mud clasts were entrained at the base of the flow, and were presumably suspended by their buoyancy and dispersive pressure in the high-concentration lower part of the flow (Postma et al., 1988). HDTs thus transition down dip into beds with increasing volumes of mudstone clasts (MRBs) which tend to accumulate progressively in higher parts of the bed vertical profile. In both HEBs and MRBs, mudstone clasts and argillaceous sandstones are always contained in the basal relatively coarse grained and mostly structureless part of the bed beneath the Tb division, whereas the finer-grained laminated part is always made of clean sandstone (Tb-e; H4 division). This observation suggests that turbulence suppression and/or an increase in flow cohesion happened in the near-bed, high-concentration part of the flow along the interface with the upper highly turbulent region (see Mutti & Nilsen, 1981 and Postma et al., 1988). The clasts can be rapidly buried by fall out of sand from suspension at the level they were able to reach as they were carried by the dense flow (Mutti & Nilsen, 1981), or accumulated at the top of the aggrading bed, where they started to move as a shearing boundary layer. Evidence of active shear includes the crude stratification of oblate mudstone clasts, occasional imbrication and deformed sand patches in a very heterogeneous sandy-matrix. Clast-to-clast friction and sand-injections extending from the overpressured sandy base of the flow were able to systematically fragment the clasts and release both mud chips and dispersed clay which mixed with the surrounding sandy matrix. Dewatering of the basal sand may have also sustained the transport of what were pseudo-cohesive flows producing a thin overpressure water layer on which the flow decoupled and hydroplaned (Haughton et al., 2009). Clast over-concentration and clay release would have progressively increased the cohesiveness of the flow forcing it to arrest *en-masse*, depositing beds with H3 divisions characterised by poorly-sorted mudstone clasts surrounded by a clay-enriched sandy matrix (HEB-3). Clast attrition would have produced progressively finer clasts

that were deposited in more distal locations resulting in HEB-4. The longitudinal and lateral transition from MRB to HEB-3 and HEB-4 can be irregular and highly variable at short-length scales due to the complex interfingering between the up-dip sandstone-dominated part of the bed and the down-dip muddier section due to pattern of concentration of clasts and clay in the flow (Fonnesu et al., 2015), or by the uneven pattern of substrate entrainment (Fonnesu et al., 2015; 2016; Southern et al., 2015). An example of this facies tract is provided by Bed 12, which preserves a 1.6 km down-flow transition from mudstone clast-poor massive turbidite bed (HDT) to a mudstone-clast rich hybrid event bed (HEB-3) via an intermediate MRB bed (Fig. 17A).

(C) FTH-2 Hybrid flow evolution via substrate rafts disaggregation

A second type of hybrid event bed facies tract (FTH-2; Fig. 18B) involves both lateral and down-dip transitions between raft-bearing and chaotic hybrid event beds (HEB-1 and HEB-2) with mudstone clast-bearing HEBs (HEB-3 and HEB-4). The up-dip equivalent bed type referred to this facies tract is uncertain, but a limited number of beds show transition from proximal coarse-grained high-density turbidites (HDTs) lacking mudstone clasts. This type of facies tract is interpreted to have been generated by flows that were able to deeply erode the underlying substrate and which were capable of detaching and transporting large pieces of remobilized stratigraphy. The mechanism of raft entrainment was probably related to a combination of lateral sand-injection and contemporaneous slab detachment, triggered by flow pressure variations or enhanced turbulence at the front of high-concentration and high-volume flows (Fonnesu et al., 2016). The evidence for erosion cutting down several metres beneath parts of some HEB-1 and HEB-2 beds (Fig. 18B), and matches between the texture and character of the rafts and the underlying substrate, suggest that the blocks were mostly sourced locally. Intact substrate rafts were presumably transported for short distances remaining relatively undeformed (HEB-1), partially ploughing into the unconsolidated basal sand (Fonnesu et al., 2015). Alternatively they may have been entrained in the flow and deformed by shear forming a chaotic texture, or partly invaded and broken up by sand-injections sourced from the basal sand (HEB-2). The basal H1 sand was probably overpressured to be able to support gliding mudstone rafts on top of the just-deposited basal sand with associated hydro-plastic

deformation of the blocks (SC facies; Fig. 6) and their lateral disaggregation as part of a shearing near-bed-layer. Both downcurrent and lateral to the entrained rafts, a mud clast rich flow, partially derived by spalling of fragments from the rafts as they disaggregated, forming HEB-3 and HEB-4 beds. A partial example of this down-flow facies transition is provided by Bed 15.4 in which a heterolithic raft-bearing bed erosively cuts though the underlying thin-bedded substrate in the most proximal section, transforming down-dip into HEB types containing smaller mudstone clasts (HEB-3) with occasional pieces of deformed stratigraphy still preserved (Fig. 17B).

(C) Distal expression of FTH-1 and 2

The normally graded and laminated capping sandstones (H4 divisions) that are developed in both facies tracts are thought to have been deposited just prior to or after the underlying H3 deposit arrested by a slower moving dilute turbulent wake of the flow. The dilute turbulent cloud can potentially have run-out further than the parent high-concentration flow and deposited down-current as a fine-grained normally graded bed (see examples of Amy et al., 2005; Amy & Talling, 2006; Muzzi Magalhaes & Tinterri, 2010; Talling et al., 2012; Fonnesu et al., 2015).

It is reasonable to think that HEB-3 or HEB-4 can transform distally into HEB-5 or HEB-6, if the flow had enough space to evolve and the process of particle disintegration, hydraulic segregation and clay release remained efficient. Examples of similar lateral transitions from very extensive basin plains are provided by Amy & Talling (2006) and Muzzi Magalhaes & Tinterri (2010). However, in the Gottero case study, this evolution is statistically insignificant. The possible reasons could be: 1) the process of clast disaggregation was not efficient enough; 2) the Mt. Ramaceto section is still relatively proximal; 3) the basin was too small and the flows did not have the space to undergo a complete evolution.

(B) Clast-poor and clay-rich hybrid event beds (HEBs 5-6)

HEB-5 and HEB-6 have a H3 division which is more depleted in mudstone clasts but enriched in pore-filling clay in comparison to the other HEB types. HEB-5 and HEB-6 appear mostly interbedded and systematically arranged in FA-B and FA-C facies associations, located in the

proximal and intermediate Gottero system sectors. Because these HEBs mostly developed in lobe settings controlled by compensational stacking, progradation or lateral switching, it is possible to infer that the systematic vertical distribution of bed thickness and bed types could represent the expression of a longitudinal and lateral bed facies tract, according to the Walther's law. A similar approach has been adopted by Middleton (1973) and Kane & Pontén (2012).

(C) FTH-3 Hybrid flow evolution via clay enrichment and fractionation

The inferred longitudinal facies tract (FTH-3; Fig. 18C), results in a progressive decrease of the H1 thickness and a simultaneous expansion of the H3 division in HEB-5 beds. It distally culminates in the reduction and pinch-out the basal sandstone (and eventually of the overlying H2 banded division), followed by distal pinch out of the H3 division. The dilute turbulent wake responsible for deposition of the graded and laminated H4 division can outrun the deposit of the hybrid flow, and settle in more distal and lateral lobe fringes. In mud-rich lobe fringe sequences, HEB-6 beds containing an argillaceous unsorted interval developed above a graded and well-structured thin bed, are commonly found and interpreted as the most distal and lateral expression of the facies tract.

The facies tract is interpreted to be the expression of the progressive deceleration and turbulence damping of a mud-enriched flow. The presence of a higher amount of organic matter in the H3 division may suggest that most of the cohesive material could be bulked in the flow in a more proximal location than in the other flow types (Hodgson, 2009). A significant amount of fines can be entrained in up-dip fan sectors at channel mouths, proximal lobes or flow expansion points (Haughton et al., 2003; 2009; Talling et al., 2004), maybe on account of hydraulic jump-related erosion (Mutti and Normark, 1987; Mutti, 1992). Alternatively, the facies tract could represent the deceleration and/or fractionation of already clay-laden flows (Haughton et al., 2003). The presence of hydraulically-fractionated flaky materials in HEB-5 beds suggests the onset of efficient longitudinal and transverse segregation of components with lower settling velocities (see Pyles et al., 2013) leading to a transitional to laminar flow conditions (Haughton et al., 2009; Kane and Pontén, 2012; Kane et al., 2017). Alternatively the same bed types could derive from the vertical

segregation of the mud components via top-down turbulence damping in a transitional flow (Sumner et al., 2009; Baas et al., 2009). This model predicts initial onset of near-bed turbulence enhancement before the turbulence is eventually damped. This is consistent with the presence of flute casts at the base of HEB-5 beds, suggesting that the basal flow was more turbulent than in the other HEB types which are dominated by tabular scours and grooves.

The occasional presence of a banded H2 division in HEB-5 beds, a feature not observed in other bed types, reflects a more gradational change in flow rheology from a turbulent flow to a transitional and then a cohesive and turbulent suppressed flow (Haughton et al., 2009; Davis et al., 2009). The facies tract predicts that the very distal expression of this kind of flow is represented by thin LDTs representing the distal run-out of the trailing turbulent wake which in the more proximal location forms the H4 division. Alternatively the flow can express further transformation recorded by the deposition of HEB-6 beds. In HEB-6, fine-grained mud-enriched sand is deposited on top of a laminated and/or rippled sandstone. The development of a further ungraded sandy, but clay-rich interval, distinctive from a normal mud cap, is interpreted to be related to vertical clay segregation leading to top-down turbulence damping and formation of a mud plug (see Baas et al., 2009; Sumner et al., 2009) in a decelerating flow (Pierce, 2015). The common presence of ripples instead of parallel lamination below the muddy unit in this kind of bed can be related to a slight turbulence enhancement due to the onset of the plug flow (Baas et al., 2009; 2011). Therefore the deposition of the mud-rich interval observed in HEB-6 beds can be interpreted as a mud-enriched flow produced by a secondary turbulence damping episode following the deposition of the trailing turbulent wake, due to the hydraulic separation of clay at the end of current runout (Pierce, 2015).

(A) DISCUSSION

(B) Hybrid event bed types distribution in Gottero system sub-environments

The two previously highlighted hybrid event bed groups (mudstone-clast rich HEBs and clast-poor HEBs) are found in different facies associations and hence different Gottero sub-environments. This pattern indicates HEB character and relative abundance is strictly dependent on

palaeogeographic location within the Gottero system. As general rule, the proximal area of the Gottero system is interpreted as a relatively unconfined fan system and mainly includes clast-poor and clay-rich hybrid event beds; the down-dip confined basin plain sectors are in contrast dominated by extensive mudstone-clast rich and raft-bearing HEBs.

The most proximal sectors of the Gottero system, including the slope channels fills, sand-prone channel lobe transition zone (FA-A), and slope deposits (FA-F), are completely devoid of hybrid event beds. HEBs have been reported in channelized or proximal fan sectors in a few cases (e.g. East Carpathian Flysch, Romania; Sylvester & Lowe, 2004; Ross Sandstone Formation, Western Ireland; Schiehallion Field, West Atlantic margin; Haughton et al., 2009; Champsaur channel complex, SE France; Vinnels et al., 2010; channelized Permian Brushy Canyon Formation, West Texas U.S.A.; Haughton et al., 2009), but are generally uncommon. This is despite the fact that substrate erosion and clast rip-up are common in these settings; however, erosion products tend to end up deposited in poorly organized mudstone-clast conglomerates rather than hybrid event beds. The clast rip-up is probably mostly linked to local erosion and bypass-lag formation. A possible explanation behind the absence of HEBs in this setting may be that the flow constriction by the channel margins or the onset of hydraulic jumps at the channel-lobe transition, could temporarily increase the flow turbulence (Talling et al., 2007; Kane et al., 2017) preventing the turbulence suppression and hybrid bed deposition until the flows were eventually able to distally expand and decelerate. The loose mud eroded from the substrate could be easily elutriated and transferred to upper turbulent cloud well away from the bed increasing the run-out of the high-density flows (Mohrig & Marr, 2003; Tinterri et al., 2003; Breien et al., 2010)., with eventual deposition downslope as mud caps.

Hybrid event beds are present in the Gottero system in mid- and outer-fan areas (comprising about 15% of the event bed inventory by thickness) where they can be found within three stratigraphic contexts. Thin HEBs (HEB-5 and 6, very rarely HEB-4) are interbedded in widespread fine-grained inter-lobe facies that alternate with thick amalgamated lobe sequences (FA-B). The mud necessary to suppress the flow turbulence could be sourced from original slope failures or by

progressive entrainment from poorly compacted substrate, providing clay and small mud chips. A second occurrence comprises clay-enriched HEBs (HEB-5 and HEB-6) that are found interbedded in lobe sequences (FA-C) as a precursor of thickening upward cycles or in thin-bedded bundles interpreted as lobe fringe deposits. These HEBs are thought to have formed from flows that entrained clay up-dip (from channel-lobe transition zones, slope or proximal lobe settings) and underwent progressive turbulence damping and deceleration in distal and lateral lobe fringes. They are thought to be genetically linked with MRBs and HDTs beds observed in the overlying axial lobe deposits. Similar models have been invoked in the Jurassic of North Sea (Haughton et al., 2003), in the Permian Karoo basin (Hodgson, 2009; Kane et al., 2017) and in the Paleogene Wilcox Formation (Kane & Pontén, 2012), in which hybrid event beds are common in the lower prograding base of lobe sequences, being the expression of distal lobe fringes. The presence of armoured mudstone clasts with sand or granules grains in the MRBs vertically associated with the HEBs suggests that at least part of the mud entrained was derived from more proximal fan areas, rather than from the local seabed erosion. A third context in mid-fan and outer-fan sectors in which hybrid event beds can be found is at the base of lobe sequences (FA-B and FA-C) directly overlying mud-rich inter-lobe deposits. In this case they are expressed as thick mudstone clasts or raft-bearing HEBs (HEB-1; HEB-2; HEB-3) which are otherwise rare in the various unconfined fan facies associations. By analogy with the hybrid event beds found in the distal confined basin plain and by the repetitive association with a muddy substrate, these beds are thought to have formed by local delamination and clast entrainment, controlled by the availability of a widespread muddy substrate, combined with the first high magnitude flows to arrive after a lobe avulsion.

In the distal areas of the Gottero system where basin topography was flat (e.g. a confining basin plain setting), an aggradational stacking pattern dominated. Here a marked change in the character of the hybrid event beds occurs. HEB-5 and 6 are very uncommon in this setting and are replaced by generally very thick and tabular, laterally-extensive hybrid event beds (HEB-1 to HEB-4). These are found as isolated beds (FA-D), or more rarely in weakly amalgamated packages (FA-C), and usually include thick mudstone caps. Similar stacking patterns have been observed in examples

located in the Castagnola ponded basin (Southern et al., 2015; Marini et al., 2016) or in the extensive foredeep basin plain of the Marnoso Arenacea (Ricci Lucchi & Valmori, 1980; Amy & Talling, 2006; Muzzi Magalhaes & Tinterri, 2010; Tinterri & Muzzi Magalhaes, 2011; Talling et al., 2012; Tinterri & Tagliaferri, 2015).

(B) Controls on hybrid event bed development in the Gottero system

The importance of external factors on the development of hybrid event beds has been stressed by a number of authors (Haughton et al., 2003; 2009; Talling et al., 2004; Hodgson et al., 2009). Non-equilibrium feeder systems or slopes (e.g. Ross et al., 1994), occurring for both stratigraphic and tectonic reasons, could cause proximal erosion and clay acquisition leading to the development of hybrid flows down-dip (Haughton et al., 2009; Muzzi Magalhaes and Tinterri, 2010; Tinterri and Muzzi Magalhaes, 2011). In tectonically quiescent basins such as the Karoo Basin (Skoorsteenberg Formation) or the Ross Sandstone Formation, western Ireland, it has been suggested that hybrid event beds generation could be related to phases of fan initiation and growth (Hodgson, 2009; Haughton et al., 2009) and controlled by relative sea level falls during early low-stand periods, with consequent increase of sediment supply, flow efficiency and hence capacity for erosion (Hodgson, 2009). A similar process can probably explain the onset of a HEB-prone package at the base of the Gottero 2 unit (Fig. 4), which marks the initiation of the sand-prone Gottero fan. Nevertheless, the Gottero system remains hybrid-prone throughout most of its history, and the variable character and abundance of hybrid event beds appears to be linked to their arrangement in different sub-environments, rather than to external factors. The Gottero hybrid events thus seem to reflect autogenic and intrabasinal factors such as lateral shifting of lobe axes and fringes, flow magnitude and type of substrate. A subsidiary control could be the physiography of the basin, in particular the onset of confined and ponded conditions towards the end of the Gottero basin fill.

(C) Lobe compensational stacking

Hybrid event beds have been recognised interbedded with prograding or laterally shifting outer-fan lobes, as part of packages interpreted as lobe fringes. Hodgson (2009) documented that hybrid event beds can be concentrated in the basal basinward-stepping phases of turbidite lobes, and be

virtually absent during retreat stages. The same pattern has been recognised at multiple scales (from lobe to fan); including HEBs concentrated in the lower part of overall prograding fan successions (Haughton et al., 2009). Nevertheless, a similar pattern has not been observed in the Gottero system, where hybrid beds are present during most of its evolution, and are not more common at any particular stratigraphic level. In the outer-fan Gottero 3 sections (Moneglia; FA-C), HEB-5 and HEB-6 beds are found within the thinner bedded portions of thickening- or thinning-upward cycles, independent of their stratigraphic level, suggesting that their occurrence is linked to the establishment of lobe off-axis or fringe facies preceding or following amalgamated lobe axis facies. Their occurrence in vertical sections is therefore only related to the lateral shifting or progradation of lobes that are constantly hybrid-prone in their fringes. The dynamic of lobe shifting could be controlled by rapid distributary channel avulsions (when there is a rapid vertical transition between coarse-grained amalgamated and thin-bedded intervals), or by lobe progradation or swinging across strike (see Prélat & Hodgson, 2013).

(C) Flow magnitude and entrainment processes

Flow volume and concentration control flow run-out distance (Mutti, 1992; Dorrell et al., 2014) and flow interaction with the sea floor (Stevenson et al., 2013), shifting basinward or landward the area of flow bypass and deposition (Mutti et al., 1994), and influencing the mechanism of mud entrainment. The Gottero system contains a wide spectrum of flow types, which deposited their sediment load in different locations (Fig. 19). 1) High-magnitude flows are thought to have generally bypassed the fan area (see Mutti & Johns, 1982; Remacha et al., 2005; Fonnesu et al., 2016), and deposited in the confined distal basin plain (high-efficiency), developing thick clast-rich HEBs (type 1 to 4). 2) Smaller volume flows that deposited the bulk of their sedimentary load in the more proximal fan system (low-efficiency), developing compensating lobes and clast-poor HEBs (type 5 and 6) in the lobe fringes close to the run-out limit. The presence of very different flow types is typical of tectonically-active basins in convergent settings (Mutti et al., 1984; Mutti et al., 2009).

High-magnitude flows are thought to be responsible for the deposition of turbidite beds of exceptionally large volume and extent (in comparison with basin size) which presumably filled the entire Gottero basin plain. Most of them deposited thick hybrid event beds attributed to types 1 to 4. Uncertainties on the location of basin boundaries do not allow a precise reconstruction of the volumes involved. However, considering the sandy part of the thickest event bed recorded in the Mt. Ramaceto section (9.5 m) and its minimum areal extension (150 km^2, but possibly much larger), the total sand volume transported could be greater than 1.3 km^3. Such high volume event beds may have been generated by catastrophic failures of the Sardo-Corsican margin which were likely triggered by earthquakes during plate convergence ("seismoturbidites" of Mutti et al., 1984). Those events were able to produce flows that mostly bypassed the more proximal fan area and deposited their sediment load in flexural basin plain depocentres producing beds several metre thick. The facies interpretation of their H1 division suggests that they were deposited by high-concentration flows. The local mud entrainment documented by the scours and the H3 character is attributed to substrate delamination rather than turbulent erosion.

Smaller volume flows formed sandstone lobes in the proximal system area, and deposited HEB-5 and HEB-6 in the related lobe fringes or interlobe intervals. Because of their relatively small volume, individual flows did not expand to fill the entire basin area, but they deposited their sediment load on the area in front of the feeder channel mouths, forming composite sandbodies showing lenticular and compensational geometries. These smaller-volume flows probably only occasionally reached the distal basin plain area where they deposited laterally extensive fine-grained low-density turbidites, forming distinctive heterolithic thin-bedded packages, but not hybrid event beds. These events were probably triggered by episodic slope failures caused by sedimentary oversteepening (Kastens, 1984; Mutti et al., 1984; Mutti, 1992), as opposed to large seismic shocks. These flows were likely of low concentration in a distal setting and hence generally did not exercise enough pressure on the substrate to trigger sea floor delamination (e.g. except when the substrate was particularly mud-prone). Instead, the mud entrainment could have been driven by turbulent erosion at the front of the current in up-dip areas, providing disaggregated

mud particles into the flow, which then suppressed the flow turbulence, resulting in deposition of hybrid event beds in the up-dip lobe region.

(C) Substrate mechanical proprieties

Evidence of substrate delamination features beneath hybrid event beds deposited on the Gottero basin floor supports the hypothesis that local substrate mechanical properties may have had a significant impact on the development of some types of hybrid event bed (Fonnesu et al., 2016). This appears to be the case for mudstone-clast rich, chaotic and raft-bearing HEBs (HEB-1 to 4) in both confined basin plain and locally in fan settings. The preservation of large and undeformed mudstone or heterolithic rafts in HEB-1 beds confirms that the sea floor from which they were derived was relatively firm and cohesive. A relatively compacted sea floor is also inferred in other confined and ponded basins (Castagnola, Southern et al., 2015; Ventimiglia Flysch, Marini et al., 2015b), An explanation could be that the distal setting with respect to their feeder system meant that only a limited number of events reached the basin plain, resulting in a lower gravity flow frequency and a greater time available for the seafloor mud to dewater and consolidate (Mutti & Johns, 1978; Mutti, 1992; Remacha et al., 2005; Fonnesu et al., 2016). As shown by Remacha et al. (2005), and confirmed by the Gottero case study, such a hypothesis is supported by the fact that the number of individual event beds present in the basin plain areas is lower than in the up-dip lobe settings, despite individual beds being thicker in the former case.

The presence of a firm sea floor does not hinder its delamination; conversely, it allows flows to detach large pieces of substrate which can be carried intact, instead of being disaggregated immediately. The delamination process could be favoured by the presence of planar mechanical weakness in the substrate formed by thin-bedded intervals, early diagenesis or by subtle fabric changes in mudstone caps (Fonnesu et al., 2016). The same kind of effect could happen also in more proximal setting when flows interact with a mud-prone substrate and produce local delamination and formation of mudstone-clast rich, chaotic or raft bearing HEBs at the base of lobe sequences.

(C) Effect of basin confinement and ponding

Basin physiography and in particular the presence of topographic highs, basin margins, or confining slopes is a major control on the development and deposition from hybrid flows (Barker et al., 2008; Davis et al., 2009; Muzzi Magalhaes & Tinterri, 2010; Patacci et al., 2014; Southern et al., 2015; Tinterri & Tagliaferri, 2015; Tinterri et al., 2017). The presence of basin floor highs and counter slopes can favour rapid flow deceleration and hence an increase in fallout rate, flow stratification and associated turbulence damping (Talling et al., 2004; Muzzi Magalhaes & Tinterri, 2010; Patacci et al., 2014). In addition, flow impact against counter slopes could focus the flow hydraulic pressure and promote substrate delamination processes by hydraulic jacking (Puigdefàbregas et al., 2004). Examples provided by Patacci et al. (2014) from the Braux Unit of the Annot sandstone of SE France illustrate that flow confinement in a relatively proximal position results in the occurrence of HEBs next to the confining slopes, with transitions from clean turbidites to HEBs occurring over short distances (i.e., few hundreds of metres). In a ponded mini-basin settings (e.g. Castagnola system of NW Italy) flows deposited relatively sandy HEBs (MRBs and HEB-3, rarely HEB-1 and HEB-2) without any systematic variation of their depositional character with respect to distance from a counter slope. Such a trend is thought to be due to complex three-dimensional flow dynamics across the enclosed basin and interaction with multiple basin margins, which inhibited the development of coherent depositional trends (Southern et al., 2015). Hovewer, based on their work on the Marnoso-areanacea, Peira Cava and Ranzano case studies, Tinterri et al., (2016; 2017), note that where flows are strongly confined (but not ponded) and the flow efficiency is low, the deposition of clay-rich HEBs is hindered, favouring the deposition of structureless beds with basal impact structures (*sensu* Mutti, 1992) or with traction reworked tops due to enhanced flow bypass

The distal and upper part of the Gottero system (Mt. Ramaceto section) was deposited in a confined and presumably ponded basin as demonstrated by the sedimentary facies and thick mudstone caps described in facies association FA-E. High-density turbidites and the basal divisions of HEBs do not record any effect of flow-slope interaction (i.e. rotation of palaeoflow

indicators, systematic trends in H3 development) indicating that the inbound underflows were relatively unaffected by the confinement conditions (Patacci et al., 2015). This suggests that the confining slopes were relatively distant (> 10 km); the counter slope was likely located near the Bracco massif of Elter & Raggi (1965) (Figs 2 and 3) and did not affect the process of substrate entrainment. The presence of HEBs including the variable expression of mudstone-clast rich H3 divisions thus cannot be linked to the effect of confining slopes on flow behaviour (c.f.. Southern et al., 2015). Furthermore, the persistence of hybrid event beds through the entire Gottero 3 history indicates they are independent of the changing degree of basin confinement.

Evidence for extensive scour features in the basin-plain region suggests that hybrid event bed occurrence in this sector (especially the mudstone-clast and raft-bearing type HEBs) was controlled by the magnitude of the flows and the type of substrate with which they interacted, rather than any up-dip erosion related to phases of tectonic uplift or slope rotation. A tectonic control would have formed a stacking pattern in which HEBs were stratigraphically partitioned, as has been inferred by Muzzi Magalheas and Tinterri (2010) and Tinterri and Muzzi Magalheas (2011) for the Marnoso arenacea. A subtle gradient break between the up-dip fan system and the oversupplied and hence flat basin plain may have played a role in localising erosion and substrate entrainment on account of turbulence enhancement followed by rapid suspension collapse. Local erosion may have formed initial defects which were then expanded by injection-related delamination (Fonnesu et al., 2016). Flow containment seems to have affected only the dilute upper part of the flows, responsible for the deposition of expanded laminated and fine-grained bed tops and the preservation and accumulation of thick mudstone caps. The basin plain area was probably the first location along the flow path where large-volume flows encountered a cohesive and well-layered muddy substrate (including thick ponded mud caps to earlier flows) forming the ideal conditions to promote delamination and mudstone-clast and raft-bearing HEB formation.

(A) CONCLUSIONS

Hybrid event bed presence and character have been documented across a range of Gottero system sub-environments in both submarine fan and confined basin plain sectors (Fig. 19).

1) Hybrid event beds can be differentiated on the basis of the texture of their H3 divisions and of the size and shape of the clasts entrained within them. Six HEB bed types can be distinguished on the following basis: beds with H3 divisions including metre to 10s of metres long substrate rafts (HEB-1); highly deformed chaotic texture or sand-injection rich (HEB-2); mudstone clast to smaller mud-chips rich in a sand-rich matrix (HEB-3 and HEB-4); and H3 division with small mud-chips scattered in a matrix with high dispersed and significant mud content (HEB-5 or HEB-6).
2) The proximal fan area of the Gottero system is virtually devoid of HEBs in channel-fill and amalgamated proximal lobe elements.
3) Thin and fine-grained HEBs (HEB-5 and 6) are abundant in the lateral and frontal fringes of outer-fan sandstone lobes and less commonly interbedded in mud-prone laterally extensive inter-lobe intervals (Fig. 19). This HEB association is thought to have been produced by flows that underwent turbulence damping following incorporation of mud from proximal lobe locations or at flow expansion points and that longitudinally hydraulically fractionated clay and other low density components. They are thought to produce a facies tract in which H3 divisions expand down-dip at expenses of their basal sandstone and may include components deposited under transitional flow conditions.
4) The Gottero confined basin plain is dominated by thick and laterally extensive event beds with a high proportion of HEBs (31% to 51% in thickness) (Fig. 19). Hybrid event beds in this case are rich in mudstone clasts and large substrate rafts (HEB-1 to HEB-4) and show evidence of extensive auto-injection and clast break-up within a sand-rich matrix. These beds are thought to have been produced by high-magnitude flows capable of delaminating the sea-floor locally and detaching pieces of substrate. On the basis of this study the process can produce two types of facies tracts: FTH-1 involving substrate erosion from shallow scours and entrainment of

abundant mudstone clasts; or FTH-2 driven by delamination of large substrate slabs and their progressive disaggregation in shearing near-bed layers.

5) The occurrence of fine-grained HEBs (HEB-5 and 6) was controlled by the vertical and lateral juxtaposition of lobes and lobe fringes which was ultimately related to the pattern of autogenic lobe stacking.

6) Clast-rich and raft-bearing HEBs relate to less frequent, large-magnitude and high-concentration flows that interacted with a cohesive substrate either immediately following deposition of muddy interlobes or beyond the fan on an oversupplied basin plain. Extensive delamination of the Gottero basin plain may have been promoted by the gradient break between the fan and the confined basin plain, and the presence of ponded mud caps on preceding event beds.

7) The Gottero turbidite system was prone to hybrid flow generation through most of its history. In this case local HEB occurrence and distribution across different sub-environments was strongly controlled by intrabasinal factors such as the availability of muddy substrate, mechanical properties of which dictated the mode of substrate entrainment.

ACKNOWLEDGMENTS

This work was founded by the Turbidites Research Group sponsors: Anadarko, BG-Group, BP, Conoco Phillips, Dana Petroleum, Hess, Eni, Nexen, OMV, Petronas, Shell, Statoil, and Woodside. Luca Baruffini is warmly acknowledged for introducing us to the Gottero outcrops and Marco Carnevale is thanked for field assistance. Also we would like to thank the editor in chief Nigel Mountney and the reviewers Ian Kane and Roberto Tinterri, whose perceptive comments helped to improve the final version of the manuscript.

REFERENCES

Abbate, E. and **Sagri, M.** (1982) Le unità torbiditiche cretaciche dell'Appennino settentrionale ed i margini continentali della Tetide. *Mememorie della Società Geologica Italiana*, **23**, 115-126.

1033 **Abbate, E.**, and **Sagri, M.** (1970) The eugeosynclinal sequences: *Sedimentary Geology*, **4**, 251-
1034 340.

1035 **Abbate, E., Bortolotti, V.** and **Principi, G.** (1980) Apennine ophiolites: a peculiar oceanic crust.
1036 *Ofioliti*, **1**, 59-96.

1037 **Amy, L.A., Talling, P.J., Peakall, J., Wynn, R.B.,** and **Thynne, R.A.** (2005) Bed geometry used
1038 to test recognition criteria of turbidites and (sandy) debrites. *Sedimentary Geology*, **179(1)**, 163-
1039 174.

1040 **Amy, L.A.** and **Talling, P.J.** (2006) Anatomy of turbidites and linked debrites based on long
1041 distance (120 × 30 km) bed correlation, Marnoso Arenacea Formation, Northern Apennines, Italy.
1042 *Sedimentology*, **53**, 161-212.

1043 **Amy, L.A., Kneller, B.C., and McCaffrey, W.D.** (2007) Facies architecture of the Grès de Peïra
1044 Cava, SE France: landward stacking patterns in ponded turbiditic basins. *Journal of the Geological*
1045 *Society*, **164**(1), 143-162.

1046 **Amy, L.A., Peatchy, S.A., Gardiner, A.A.** and **Talling, P.J.** (2009) Prediction of hydrocarbon
1047 recovery from turbidite sandstones with linked-debrite facies: Numerical flow-simulation studies.
1048 *Marine and Petroleum Geology*, **26**, 2032-2043.

1049 **Andri, E.**, and **Zavatteri, F.** (1990) Le septarie di Monte Mignano e de il Dente (Complesso di
1050 Monte Ramaceto, Appennino Ligure). *Atti Società Toscana Scienze Naturali*, **96**, 1-48.

1051 **Arfaie, A., Burns, A.D., Dorrell, R.M., Eggenhuisen, J.T., Ingham, D.B.,** and **McCaffrey,**
1052 **W.D.** (2014) Optimised mixing and flow resistance during shear flow over a rib roughened
1053 boundary. *International Communications in Heat and Mass Transfer*, **58**, 54-62.

1054 **Baas, J.H., Best, J.L.** and **Peakall, J.** (2011) Depositional processes, bedform development and
1055 hybrid bed formation in rapidly decelerated cohesive (mud-sand) sediment flows. *Sedimentology*,
1056 **58**, 1953-1987.

Baas, J.H., Best, J.L., Peakall, J. and **Wang, M.** (2009) A phase diagram for turbulent, transitional, and laminar clay suspension flows. *Journal of Sedimentary Research*, **79**, 162-183.

Barker, S.P, Haughton, P.D.W., McCaffrey, W.D., Archer, S.G. and **Hakes, B.** (2008) Development of rheological heterogeneity in clay-rich high-density turbidity currents: Aptian Britannia sandstone member, U.K. Continental shelf. *Journal of Sedimentary Research*, **78**, 45-68.

Bortolotti, V., and **Passerini, P.** (1970) Magmatic activity. *Sedimentary Geology*, **4**, 599-624.

Bouma, A.H. (1962) Sedimentology of some Flysch deposits; a graphic approach to facies interpretation. Amsterdam, Elsevier, 168 p.

Breien, H., De Blasio, F. V., Elverhøi, A., Nystuen, J.P., and **Harbitz, C.B.** (2010) Transport mechanisms of sand in deep-marine environments—insights based on laboratory experiments. *Journal of Sedimentary Research*, **80(11)**, 975-990.

Brunt, R. L., Di Celma, C.N., Hodgson, D.M., Flint, S.S., Kavanagh, J.P., and **van der Merwe, W.C.** (2013) Driving a channel through a levee when the levee is high: an outcrop example of submarine down-dip entrenchment. *Marine and Petroleum Geology*, **41**, 134-145.

Casnedi, R. (1982) Sedimentazione e tettonica della unità liguri nell'Appennino nord-occidentale (Valli Lavagna-Sturla Trebbia e Aveto). *Atti Istituto Geologico Università di Pavia*, **30**, 42-66.

Costa, J.E. (1984) Physical geomorphology of debris flows. *In* Developments and applications of geomorphology, pp. 268-317. Springer Berlin Heidelberg

Davis, C.E., Haughton, P.D.W., McCaffrey, W.D., Scott, E., Hogg, N. and **Kitching, D.** (2009) Character and distribution of hybrid sediment gravity flow deposits from the outer Forties Fan, Palaeocene Central North Sea, UKCS. *Marine and Petroleum Geology*, **26**, 1919-1939.

Dorrell, R.M., Darby, S. E., Peakall, J., Sumner, E.J., Parsons, D.R., and **Wynn, R.B.** (2014) The critical role of stratification in submarine channels: Implications for channelization and long runout of flows. *Journal of Geophysical Research: Oceans*, **119(4)**, 2620-2641.

Elter, P., and **Raggi, G.** (1965) Contributo alla conoscenza dell'Appennino ligure, 3. Tentativo di interpretazione delle brecce ofiolitiche cretacee in relazione con movimenti orogenetici nell'Appennino ligure. *Bollettino della Società Geologica Italiana*, **84**, 1-12.

Elter, P., Ghiselli, F., Marroni, M. and **Ottria, G.** (1997) Note illustrative della Carta geologica d'Italia alla scala 1: 50.000, Foglio 197-Bobbio. Istituto Poligrafico e Zecca dello Stato, Roma.

Flemings, P.B., Behrmann, J.H., and **Johm, C.M.** (2006) Gulf of Mexico Hydrogeology. *Proceedings of the International Ocean Drilling Program*, **308**. College Station, Texas, USA.

Fonnesu, M. (2016) Hybrid event bed processes, facies trends and distribution in deep-water turbidite systems. Ph.D thesis, University College Dublin, Ireland.

Fonnesu, M., Felletti, F., Haughton, P.D.W., McCaffrey, W.D. and **Patacci M.** (2013) Bed by bed correlations and lateral variability in hybrid event beds in the Ramaceto area (Gottero Sandstone, northern Apennines, Italy), *Journal of Mediterranean Earth Sciences*, **5**, 63.

Fonnesu, M., Haughton, P., Felletti, F., and **McCaffrey, W.D.** (2015) Short length-scale variability of hybrid event beds and its applied significance. *Marine and Petroleum Geology*, **67**, 583-603.

Fonnesu, M., Patacci, M., Haughton, P.D.W., Felletti, F., and **McCaffrey, W.D.** (2016) Hybrid Event Beds Generated By Local Substrate Delamination On A Confined-Basin Floor. *Journal of Sedimentary Research*, **86**, 929-943.

Haughton, P.D.W. (2001) Contained turbidites used to track sea bed deformation and basin migration, Sorbas Basin, south-east Spain. *Basin Research*, **13**, 117-139.

Haughton, P.D.W., Barker, S.P., and **McCaffrey, W.D.** (2003) "Linked" debrites in sand-rich turbidite systems – origin and significance. *Sedimentology*, **50**, 459-482.

Haughton, P.D.W., Davis, C.E. and **McCaffrey, W.D.** (2010). Reply to Comment by R. Higgs on "Hybrid sediment gravity flow deposits – classification, origin and significance". *Marine and Petroleum Geology*, **27**, 2066-2069.

Haughton, P.D.W., Davis, C.E., McCaffrey, W.D. and **Barker, S.** (2009) Hybrid sediment gravity flow deposits – Classification, origin and significance. *Marine and Petroleum Geology*, **26**, 1900-1918.

Hodgson, D.M. (2009) Distribution and origin of hybrid beds in sand-rich submarine fans of the Tanqua depocentre, Karoo Basin, South Africa. *Marine and Petroleum Geology*, **26**, 1940-1956.

Kane, I.A., and **Pontén, A.S.M.** (2012) Submarine transitional flow deposits in the Paleogene Gulf of Mexico. *Geology*, **40**, 1119-1122.

Kane, I., Pontén, A., Vangdal, B., Eggenhuisen, J., Hodgson, D. M., and **Spychala, Y. T.**, 2017. The stratigraphic record and processes of turbidity current transformation across deep□marine lobes. *Sedimentology*. DOI: 10.1111/sed.1234.

Kastens, K.A. (1984) Earthquakes as a triggering mechanism for debris flows and turbidites on the Calabrian Ridge. *Marine Geology*, **55(1-2)**, 13-33.

Knaust, D., Warchol, M., and **Kane, I.A.** (2014) Ichnodiversity and ichnoabundance: Revealing depositional trends in a confined turbidite system. *Sedimentology*, **61**(7), 2218-2267

Kneller, B.C (1995) Beyond the turbidite paradigm: physical models for deposition of turbidites and their implication for reservoir prediction. In: Hartley, A.J. and Prosser, D.J. (Eds). Characterization of Deep Marine Clastic Systems. *Geological Society of London Special Publication*, **94**, 31-49.

Kneller, B.C., and **Branney, M.J.** (1995) Sustained high□density turbidity currents and the deposition of thick massive sands. *Sedimentology*, **42(4)**, 607-616.

Kneller, B., and **McCaffrey, W.D.** (1999) Depositional effects of flow nonuniformity and stratification within turbidity currents approaching a bounding slope: deflection, reflection, and facies variation. *Journal of Sedimentary Research*, **69(5)**, 980-991.

Kneller, B.C., and **McCaffrey, W.D.** (2003) The interpretation of vertical sequences in turbidite beds: the influence of longitudinal flow structure. *Journal of Sedimentary Research*, **73**, 706-713.

Lowe, D.R. and **Guy, M.** (2000) Slurry□flow deposits in the Britannia Formation (Lower Cretaceous), North Sea: a new perspective on the turbidity current and debris flow problem. *Sedimentology*, **47(1)**, 31-70.

Lowe, D. R. (1982) Sediment gravity flows: II Depositional models with special reference to the deposits of high-density turbidity currents. *Journal of Sedimentary Research*, **52(1)**, 272-297.

Macdonald, H.A., Peakall, J., Wignall, P.B., and **Best, J.** (2011) Sedimentation in deep-sea lobe-elements: implications for the origin of thickening-upward sequences. *Journal of the Geological Society*, **168(2)**, 319-332.

Malesani, P. (1966) Ricerche sulle arenarie, XV; L'Arenaria Superiore. *Rendiconti della Società Italiana di Mineralogia e Petrologia*, **22**, 113-175.

Marini, M., Milli, S., Ravnås, R., and **Moscatelli, M.** (2015a) A comparative study of confined vs. semi-confined turbidite lobes from the Lower Messinian Laga Basin (Central Apennines, Italy): Implications for assessment of reservoir architecture. *Marine and Petroleum Geology*, **63**, 142-165.

Marini, M., Patacci, M., Felletti, F., Cerliani, A., Azzarone, M., Decarlis, A., McCaffrey W.D. (2015b) The depositional architecture of Mass Transport Deposits from the Ventimiglia Flysch Fm. (Eocene, NW Italy): implications for seafloor reshaping and turbidite deposition. IAS meeting Krakov 22-25 June 2015.

Marini, M., Patacci, M., Felletti, F. and **McCaffrey, W D.** (2016) Fill to spill stratigraphic evolution of a confined turbidite mini-basin succession, and its likely well bore expression: The Castagnola Fm, NW Italy. *Marine and Petroleum Geology*, **69**, 94-111.

Marini, M. (1991) Considerations on the sandstone bodies of the Mount Gottero Unit west of the Bracco Massif (Ligurian Apennines, Italy). *Giornale di Geologia*, **53(2)**, 207-218.

Marini, M. (1994) Le arenarie del M. Gottero nella sezione del M. Ramaceto (unita del M. Gottero, Appennino Ligure). *Bollettino della Società Geologica Italiana*, **113(2)**, 283-302.

Marini, M. (1995) Le arenarie del Monte Gottero nell'areale del Monte Zatta (Unità del Monte Gottero, Appennino Ligure). *Bollettino della Società Geologica Italiana*, **114**, 575-598.

Marroni, M. (1991) Deformation history of the M.Gottero Unit (Internal Ligurid Units, Northern Apennines). *Bollettino della Società Geologica Italiana*, **110**, 727-736.

Marroni, M. and **Perilli, N.** (1990) The age of the ophiolite sedimentary cover from the Mt. Gottero Unit (Internal Ligurid Units, Northern Apennines): new data from calcareous nannofossils. *Ofioliti*, **15(2)**, 251-267.

Marroni, M., and **Pandolfi, L.** (2001). Debris flow and slide deposits at the top of the Internal Liguride ophiolitic sequence, Northern Apennines, Italy: A record of frontal tectonic erosion in a fossil accretionary wedge. *Island Arc*, **10**, 9-21.

Marroni, M., and **Pandolfi, L.** (2007) The architecture of an incipient oceanic basin: a tentative reconstruction of the Jurassic Liguria-Piemonte basin along the Northern Apennines–Alpine Corsica transect. *International Journal of Earth Sciences*, **96(6)**, 1059-1078.

Marroni, M., Meneghini, F. and **Pandolfi, L.** (2010) Anatomy of the Ligure-Piemontese subduction system: evidence from Late Cretaceous–middle Eocene convergent margin deposits in the Northern Apennines, Italy. *International Geology Review*, **52(10-12)**, 1160-1192.

Marroni, M., Meneghini, F., and **Pandolfi, L.** (2004) From accretion to exhumation in a fossil accrectionary wedge: a case history from Gottero unit (Northern Apennines, Italy). *Geodinamica Acta*, **17**, 41-53.

Marroni, M., Molli, G., Ottria, G., and **Pandolfi, L.** (2001) Tectono-sedimentary evolution of the External Liguride units (Northern Apennines, Italy): insights in the pre-collisional history of a fossil ocean-continent transition zone. *Geodinamica Acta*, **14(5)**, 307-320.

Marroni. M. (1994) Deformation path of the Internal Ligurid Units (Northern Apennines, Italy): record of shallow-level underplating in the Alpine accretionary wedge. *Memorie della Società Geologica Italiana*, **48**, 179-194.

Middleton, G.V. (1973) Johannes Walther's law of the correlation of facies. *Geological Society of America Bulletin*, **84(3)**, 979-988.

Mohrig, D., and **Marr, J.G.** (2003) Constraining the efficiency of turbidity current generation from submarine debris flows and slides using laboratory experiments. *Marine and Petroleum Geology*, **20(6)**, 883-899.

Monechi, S., Treves, B., and **Marri, C.** (1984) Osservazioni sell'eta'delle arenarie del Gottero; dati del nannoplancton calcareo. *Ofioliti*, **9(1)**, 93-96.

Mulder, T. and **Alexander, J.** (2001) The physical character of subaqueous sedimentary density flows and their deposits. *Sedimentology*, **48**, 269-299.

Mutti, E. and **Nilsen, T.H.** (1981) Significance of intraformational rip-up clasts in deep-sea fan deposits. Int. Assoc. Sedimentol. 2nd Eur. Regional Mtg. Abstr., Bologna, 117-l.

Mutti, E. and **Ricci Lucchi, F.** (1972) Le torbiditi dell'Appennino settentrionale: introduzione all'analisi di facies. *Memorie della Societa Geologica Italiana*, **11(2)**, 161-199.

Mutti, E. (1992) Turbidite sandstones. Agip, Istituto di geologia, Università di Parma.

Mutti, E., and **Ghibaudo, G.** (1972) Un esempio di torbiditi di conoide sottomarina esterna: le Arenarie di San Salvatore (Formazione di Bobbio, Miocene) nell'Appennino di Piacenza. *Accademia delle scienze Torino*, **4**, 16, 1-40.

Mutti, E., and **Johns, D.R.** (1978) The role of sedimentary bypassing in the genesis of fan fringe and basin plain turbidites in the Hecho Group System (south-central Pyrenees). *Memorie della Società Geologica Italiana*, **18**, 15-22.

Mutti, E., and **Normark, W.R.** (1987) Comparing examples of modern and ancient turbidite systems: problems and concepts. *in* Marine clastic sedimentology, pp. 1-38. Springer Netherlands.

Mutti, E., and **Normark, W.R.** (1991) An integrated approach to the study of turbidite systems. *in* Seismic facies and sedimentary processes of submarine fans and turbidite systems, pp. 75-106. Springer New York.

Mutti, E., and **Sonnino, M.** (1981) Compensation cycles: a diagnostic feature of turbidite sandstone lobes. In Int. Ass. Sed. 2nd European Meeting, Bologna, Abstracts, 120-123.

Mutti, E., Bernoulli, D., Ricci Lucchi, F. and **Tinterri, R.** (2009). Turbidites and turbidity currents from Alpine 'flysch' to the exploration of continental margins. *Sedimentology*, **56**, 267-318.

Mutti, E., Nilsen, T.H., and **Ricci Lucchi, F.** (1978) Outer fan depositional lobes of the Laga Formation (upper Miocene and lower Pliocene), East-Central Italy, *in* Stanley, D.J. and Kelling, G. (Eds.) Sedimentation in submarine canyons, fans, and trenches, pp. 210-222. Stroudsburg, Pa., United States, Dowden, Hutchinson & Ross, Inc.

Mutti, E., Ricci Lucchi, F., Seguret, M., and **Zanzucchi, G.** (1984) Seismoturbidites: a new group of resedimented deposits. *Marine Geology*, **55(1)**, 103-116.

Mutti, E., Davoli, G., Mora, S. and **Papani, L.** (1994) Internal stacking patterns of ancient turbidite systems from collisional basins. In: Weimer, P., Bouma, A.H. and Perkins, B.F. (Eds).

GCSSEPM Foundation 15th Annual Research Conference, Submarine Fans and Turbidite Systems: Sequence Stratigraphy, Reservoir Architecture and Production Characteristics, Gulf of Mexico and International, 257-268.

Mutti, E., Tinterri, R., Benevelli, G., di Biase, D., and **Cavanna, G.** (2003) Deltaic, mixed and turbidite sedimentation of ancient foreland basins. *Marine and Petroleum Geology*, **20(6)**, 733-755.

Muzzi Magalhaes, P. and **Tinterri, R.** (2010) Stratigraphy and depositional setting of slurry and contained (reflected) beds in the Marnoso-arenacea Formation (Langhian-Serravallian) Northern Apennines, Italy. *Sedimentology*, **57**, 1685-1720.

Nilsen, T.H. and **Abbate, E.** (1984) Submarine-Fan facies associations of the Upper Cretaceous and Paleocene Gottero Sandstone, Ligurian Apennines, Italy. *Geo-Marine Letters*, **3**, 193-197.

Pandolfi, L. (1996) Le arenarie del M. Gottero nella sezione di punta Mesco (Campaniano sup.-Paleocene inf., Appennino settentrionale): analisi stratigrafica e petrografica della parte prossimale di un sistema torbiditico. *Atti Società Toscana Scienze Naturali*, Memorie, A, **103**, 197-208.

Pandolfi, L. (1997) Stratigrafia ed evoluzione strutturale delle succession torbiditiche cretacee della Liguria orientale (Appennino Settentrionale). PhD thesis, Università di Pisa, 175 pp.

Parea, G.C. (1965) La provenienza dei clastici dell'arenaria del M.Gottero. *Atti e Memorie Accademia Nazionale di Scienze Lettere e Arti di Modena*, 6, 7 pp.

Passerini, P. and **Pirini, C.** (1964) Microfaune paleoceniche nella formazione dell'Arenaria del M. Ramaceto e degli Argilloscisti di Cichero. *Bollettino della Società Geologica Italiana*, **83**, 211-218.

Patacci, M., Haughton, P.D.W., and **McCaffrey, W.D.** (2014) Rheological complexity in sediment gravity flows forced to decelerate against a confining slope, Braux, SE France. *Journal of Sedimentary Research*, **84**, 270-277.

Patacci, M., Haughton, P.D.W., and **McCaffrey, W.D.** (2015) Flow behavior of ponded turbidity currents. *Journal of Sedimentary Research*, **85**, 885-902.

Pickering, K.T., and **Hiscott, R.N.** (1985) Contained (reflected) turbidity currents from the Middle Ordovician Cloridorme Formation, Quebec, Canada: an alternative to the antidune hypothesis. *Sedimentology*, **32(3)**, 373-394.

Pickering, K.T., and **Hiscott, R.N.** (2015) Deep Marine Systems: Processes, Deposits, Environments, Tectonics and Sedimentation. American Geophysical Union, Wiley, 672 pp.

Pierce, C. (2015) Development, distribution and evolution of gravity flows processes in the Pennsylvanian Ross Formation, Western Ireland. Ph.D thesis. University College Dublin.

Pierson, T.C. (1981) Dominant particle support mechanisms in debris flows at Mt Thomas, New Zealand, and implications for flow mobility. *Sedimentology*, **28(1)**, 49-60.

Porten, K.W., Kane, I.A., Warchoł, M.J., and **Southern, S.J.** (2016) A Sedimentological Process-Based Approach To Depositional Reservoir Quality of Deep-Marine Sandstones: An Example From the Springar Formation, Northwestern Vøring Basin, Norwegian Sea. *Journal of Sedimentary Research*, **86(11)**, 1269-1286.

Postma, G., Nemec, W., and **Kleinspehn, K.L.** (1988) Large floating clasts in turbidites; a mechanism for their emplacement. *Sedimentary Geology*, **58**, 47-61.

Prélat, A., and **Hodgson, D.M.** (2013) The full range of turbidite bed thickness patterns in submarine lobes: controls and implications. *Journal of the Geological Society*, **170(1)**, 209-214.

Prélat, A., Covault, J.A., Hogdson, D.M., Fildani, A. and **Flint, A.A.** (2010) Intrinsic controls on the range of volumes, morphologies, and dimension of submarine lobes. *Sedimentary Geology*, **232**, 66-76.

Puigdefàbregas, C., Gjelberg, J., and **Vaksdal, M.** (2004) The Grès d'Annot in the Annot syncline: outer basin-margin onlap and associated soft-sediment deformation. *Geological Society*, London, Special Publications, 221(1), 367-388.

Pyles, D.R., Straub, K.M., and **Stammer, J.G.** (2013) Spatial variations in the composition of turbidites due to hydrodynamic fractionation. *Geophysical Research Letters*, **40(15)**, 3919-3923.

Remacha, E., Fernandez, L.P., and **Maestro, E.** (2005) The transition between sheet-like lobe and basin-plain turbidites in the Hecho Basin (South-Central Pyrenees, Spain). *Journal of Sedimentary Research*, **75**, 798-819.

Ricci Lucchi, F. and **Valmori, E.** (1980) Basin-wide turbidites in a Miocene, over-supplied deep-sea plain: a geometrical analysis. *Sedimentology*, **27**, 241-270.

Ross, W.C., Halliwell, B.A., May, J.A., Watts, D.E., and **Syvitski, J.P.M.** (1994) Slope readjustment: a new model for the development of submarine fans and aprons. *Geology*, **22(6)**, 511-514.

Sagri, M. (1974) Rhythmic sedimentation in deep-sea carbonate turbidites (Monte Antola Formation, Northern Apennines). *Bollettino della Societa Geologica Italiana*, **93(4)**, 1013-1027.

Smith, G.A. (1986) Coarse-grained nonmarine volcaniclastic sediment: Terminology and depositional process. *Geological Society of America Bulletin*, **97(1)**, 1-10.

Southern, S.J., Patacci, M., Felletti, F., and **McCaffrey, W.D.** (2015) Influence of flow containment and substrate entrainment upon sandy hybrid event beds containing a co-genetic mud-clast-rich division. *Sedimentary Geology*, **321**, 105-122.

Spychala, Y.T., Hodgson, D.M., Prélat, A., Kane, I.A., Flint, S.S., and **Mountney, N.P.** (2017) Frontal and lateral submarine lobe fringes: comparing sedimentary facies, architecture and flow processes. *Journal of Sedimentary Research, **87**, 75-96.*

Stevenson, C.J., Talling, P. J., Wynn, R.B., Masson, D.G., Hunt, J.E., Frenz, M., and **Cronin, B.T.** (2013) The flows that left no trace: Very large-volume turbidity currents that bypassed sediment through submarine channels without eroding the sea floor. *Marine and Petroleum Geology*, **41**, 186-205.

Sumner, E.J., Talling, P.J., and **Amy, L.A.** (2009) Deposits of flows transitional between turbidity current and debris flow. *Geology*, **37(11)**, 991-994.

Sylvester, Z., and **Lowe, D.R.** (2004) Textural trends in turbidites and slurry beds from the Oligocene flysch of the East Carpathians, Romania. *Sedimentology*, **51(5)**, 945-972.

Talling, P.J. (2013) Hybrid submarine flows comprising turbidity current and cohesive debris flow: Deposits, theoretical and experimental analyses, and generalized models. *Geosphere*, **9**, 460-488.

Talling, P.J., Amy, L.A., Wynn, R.B., Peakall J., and **Robinson, M.** (2004) Beds comprising debrite sandwiched within co-genetic turbidite: origin and widespread occurrence in distal depositional environments. *Sedimentology*, **51**, 163-194.

Talling, P.J., Wynn, R.B., Masson, D.G., Frenz, M., Schiebel, R., Akhmetzhanov, A., Dallmeier-Tiessen, S., Benetti, S., Weaver, P.P.E., Georgiopoulou, A., Hotz, C., Cronin, B.T. and **Amy, L.A.** (2007) Debris flow deposition from giant submarine flow begins far away from original landslide, *Nature*, **450**, 541–544.

Talling, P.J., Malgesini, G., Sumner, E.J., Amy, L.A., Felletti, F., Blackbourn, G., Nutt, C., Wilcox, C., Harding, I.C., and **Akbari, S.** (2012) Planform geometry, stacking pattern, and extrabasinal origin of low strength and intermediate strength cohesive debris flow deposits in the Marnoso-arenacea Formation, Italy. *Geosphere*, **8**, 1207-1230.

Talling, P.J., Malgesini, G., and **Felletti, F.** (2013) Can liquefied debris flows deposit clean sand over large areas of sea floor? Field evidence from the Marnoso-arenacea Formation, Italian Apennines. *Sedimentology*, **60**, 720-762.

Talling, P.J., Wynn, R.B., Rixon, R., Schmidt, D., Sumner, E. and **Amy, L.A.** (2010) How did submarine flows transport boulder sized mud clasts to the fringes of the Mississippi Fan? *Journal of Sedimentary Research*, **80**, 829–851.

Terlaky, V. and **Arnott, R.W.C.** (2014) Matrix-rich and associated matrix-poor sandstones: Avulsion splays in slope and basin-floor strata. *Sedimentology*, **61**. 1175-1197.

Tinterri, R. and **Tagliaferri, A.** (2015) The syntectonic evolution of foredeep turbidites related to basin segmentation: Facies response to the increase in tectonic confinement (Marnoso-arenacea Formation, Miocene, Northern Apennines, Italy). *Marine and Petroleum Geology*, **67**, 81-110.

Tinterri, R., Muzzi Magalhaes, P.M., Tagliaferri, A. and **Cunha, R.S.** (2016) Convolute laminations and load structures in turbidites as indicators of flow reflections and decelerations against bounding slopes. Examples from the Marnoso-arenacea Formation (northern Italy) and Annot Sandstones (south eastern France). *Sedimentary Geology,* **344**, 382-407.

Tinterri, R., Laporta, M., and **Ogata, K.** (2017) Cross-currents turbidite facies tract in a structurally-confined asymmetrical mini-basin (Priabonian-Rupelian, Ranzano Sandstone, northern Apennines, Italy). *Sedimentary Geology*. Doi: 10.1016/j.sedgeo.2016.12.005.

Tinterri, R., 2011. Combined flow sedimentary structures and the genetic link between sigmoidal- and hummocky-cross stratification. *GeoActa*, **10(4)**, 1-43.

Tinterri, R., and **Muzzi Magalhaes, P.** (2011) Synsedimentary structural control on foredeep turbidites: An example from Miocene Marnoso-arenacea Formation, Northern Apennines, Italy. *Marine and Petroleum Geology*, **28**, 629-657.

Tinterri, R., Drago, M., Consonni, A., Davoli, G., and **Mutti, E.** (2003) Modelling subaqueous bipartite sediment gravity flows on the basis of outcrop constraints: first results. *Marine and Petroleum Geology*, **20(6)**, 911-933.

Valloni, R., and **Zuffa, G.G.** (1981) Detrital modes of arenaceous formations of the Northern Apennines. International Association of Sedimentologists. In 2nd European Regional Meeting, Bologna, 1981, Abstracts (pp. 198-201).

Van de Kamp, P.C. and **Leake, B.E.** (1995) Petrology and geochemistry of siliciclastic rocks of mixed feldspatic and ophiolitic provenance in Northern Apennines, Italy. *Chemical Geology*, **122**, 1-20.

Van Vliet, A. (1978) Early Tertiary deepwater fans of Guipuzcoa, northern Spain. Sedimentation in Submarine canyons, fans and trenches, 190-209.

Vescovi, P., Andreozzi, M., de Nardo, M.T., Lasagna, S., Martelli, L., Rio, D., and **Vernia, L.** (2002) Note Illustrative della Carta Geologica d'Italia alla scala 1: 50,000, Foglio 216 "Borgo Val di Taro". Presidenza del Consiglio dei Ministri, Servizio Geologico d'Italia, Regione Emilia-Romagna.

Vinnels, J.S., Butler, R.W., McCaffrey, W.D., and **Lickorish, W.H.** (2010) Sediment distribution and architecture around a bathymetrically complex basin: an example from the eastern Champsaur Basin, SE France. *Journal of Sedimentary Research*, **80(3)**, 216-235.

CAPTIONS

Fig. 1. Different styles of hybrid event bed distribution in turbidite systems, based on published examples. (A) Hybrid event beds in distributive lobe systems (modified from Hodgson, 2009) and their vertical arrangement in 1D logs at the base of prograding lobes (Kane & Pontén, 2012). (B) Hybrid event beds in confined basin plains (based on stratigraphic cross-section of Unit 3 of Miocene Marnoso-arenacea Formation, *sensu* Tinterri and Muzzi Magalhes, 2011, from Talling et al., 2012 in the interval below the Contessa key bed); the synthetic vertical log shows the lack of vertical organization of hybrid event beds and conventional turbidites at c. 20 m scale.

Fig. 2. - Location map of the Gottero system (modified from Nilsen & Abbate, 1984) and sketch map showing the tectonic units of the Northern Apennines (modified from Elter et al., 1992). The

arrows in the location map indicate the main palaeocurrent pattern deduced by Nilsen & Abbate (1984).

Fig. 3. (A) Simplified geological map of the Western Gottero study area (modified from Marroni, 1994) showing the location of measured sections (1 to 6) and palaeocurrent roses obtained during this study; the numbers in brackets indicate the number of palaeocurrent measurements. The palaeoflow pattern broadly corresponds to that established by Nilsen & Abbate (1984) (see Fig. 2). (B) Internal Liguridi stratigraphy of the Gottero tectonic unit (modified from Marroni et al., 2001). The colours on the map correspond to those displayed in the stratigraphic log.

Fig. 4. General NW-SE cross-section of the Gottero system aligned in a direction approximately parallel to the sediment transport. Colour shading according to the major grain-size and lithofacies (red colours: conglomerate and coarse grained sandstones, green: hybrid event beds, grey: mostly siltstone and mudstones or fine-grained sandstones, pink: mass transport complexes). The area interpreted as confined basin plain is coloured in light grey on the correlation panel. Note the distances between sections have not been palinspastically restored and could potentially be longer than indicated.

Fig. 5. Exposure of the upper stratigraphic part of the Gottero Sandstone in the Mt. Ramaceto area. Note the succession is tectonically inverted (arrow indicates succession way-up). Numbers refer to photohorizons highlighted in the correlation panel of Fig. 13. Orange colour represents the outcrop of the stratigraphically overlying Giaiette mass transport complex unit (MTC). The picture capture about 2.2 km lateral exposure and 740 m of stratigraphic thickness.

Fig. 6. Hybrid event bed classification scheme. Typical bed profiles (with average bed thicknesses) and photo examples. Arrows indicate the way-up when bedding is inverted (b, base of the bed; t, top of the bed).. Typical H3 sub-facies are indicated in the boxes. HEB-1 and HEB-2 can contain H3 divisions of two types: RI and MCI sub-facies can be made of undeformed or deformed mudstone rafts; SP and SC sub-facies can include undeformed pieces of thin-bedded stratigraphy or their deformed equivalents respectively. MCB: densely packed mudstone clasts (average over 5

cm) surrounded by dirty sandstone; MCD: small (2-5 cm) mudstone clasts in a dirty sandstone matrix; MDC: argillaceous sandstone with scatter mudstone clasts; MD: argillaceous sandstone without mud-chips.

Fig. 7. Petrographic and textural characteristics of the H3 division in the Gottero hybrid event beds. Samples are from HEB-3 and HEB-5 event beds located in Mt. Ramaceto and Moneglia sections respectively. The dispersed clay content (counted 500 points per section) reaches 20% in the first sample and 27% in the latter. In the HEB-3 sample mud chips are captured in the act of being partially disaggregated and contributing mud to the matrix.

Fig. 8. Thickness characteristics of hybrid event beds. (A) Box-plot showing the direct correlation between average, maximum and minimum thickness of the sandy portion (H1 to H4) of the bed, and the type of hybrid event bed. (B) Box-plot displaying the lack of correlation between the hybrid event bed type and the H1/H3 ratio, HEB-3s have the higher variability.

Fig. 9. Sandy facies associations and related interpreted depositional environments identified in the Gottero Sandstone and event bed percentages. Sedimentological logs represent examples of stacking patterns for each facies association. Pie charts show the relative abundance of bed types (for number of events and in thickness) and hybrid event bed types for each facies association (in thickness). St%: sandstone percentage of the facies association. Debrites (DEBs) and gravelly high-density turbidites (GHDTs), and low-density turbidites (LDTs) and limestones (L) categories are merged together in the statistics.

Fig. 10. Mid-fan amalgamated lobe facies and stacking patterns. (A) Representative log and typical bed types of Gottero mid-fan amalgamated lobe deposits (from the Moneglia locality, see location in Fig. 3). (B) Gottero 2 mid-fan lobes in the Mt. Ramaceto section: despite being grouped in the same facies association, the beds are slightly less amalgamated and finer grained than in the Moneglia or Deiva Marina examples. (C) Amalgamated coarse-grained sandstone beds in Moneglia showing slightly erosive bases on the underlying deposits. (D) Poorly sorted coarse-grained bed in Moneglia. (E) Granule-armoured mudstone clast. (F) Conglomeratic lenticular bed

draped by fine-grained and rippled bed (Moneglia). (G) Thin and fine-grained HEB-5 bed in mud-prone inter-lobe deposits. Way-up is indicated by arrows and by b (base) and t (top) labels.

Fig. 11. Outer-fan lobe architecture in Moneglia (Punta Baffe locality). (A) Cliff exposure of Gottero 3 sandstone; numbers represent surfaces across which changes in stacking pattern occur. (B) Close-up of the logged section displaying a 20 m thick thickening and thinning cycle. (C) Three smaller-scale thickening upward cycles in the intermediate part of the section in which thin HEBs are concentrated at the bases. Way-up to the right in B and C. Bed thickness trends are indicated by triangles.

Fig. 12. Outer-fan lobes facies and related stacking pattern. (A) Representative log and bed types of the Gottero outer-fan lobes (from Moneglia locality, see location in Fig. 3). (B) Example of HEB-5 interbedded with thin-bedded lobe fringe deposit at the base of a lobe cycle. (C) HEB-5 including a well-developed H2 banded division. (D) Poorly sorted mudstone-clast rich bed (MRB) in Moneglia lobe deposits. (E) Poorly sorted coarse-sandstone texture with small scattered angular mudstone clasts (Terrarossa section; location in Fig. 3). (F) Thin HEB-5 bed interbedded in lobe fringe deposits including a thin H2 banded interval and a rippled H4 division. All beds examples are right way-up (b: base; t: top).

Fig. 13. Architecture and stacking pattern of the Gottero 3 succession in the Mt. Ramaceto area including FA-D and FA-E facies associations (modified from Fonnesu et al., 2013). (A) Correlation panel of the upper Gottero succession from eight logs spaced over 4 km laterally. The turbiditic succession is overlain by a >300 m thick chaotic level (Giaiette shales) emplaced by mass transport processes. The base of the mass transport complex records the erosion of more than 250 m of turbiditic succession over less than 2.5 km laterally. The numbers refer to the photohorizons shown in Fig. 5, and to other labelled beds. The datum is taken at a distinctive mud-prone level rich in diagenetic carbonate nodules ("Septarie lavel" of Andri and Zavatteri, 1990). Three units bounded by mud-prone intervals (Gottero 3a, 3b, 3c; GOT3a-3b-3c) are distinguished on the basis of a progressive upward increase of sedimentological characteristics indicating an

increase in the degree of flow ponding (see text for details). Red boxes represent areas covered by the detailed correlation panels of Fig. 16. (B) Simplified outcrop map showing the position of the measured sections, the bed strikes and dips and the boundaries of the stratigraphic units.

Fig. 14. Vertical and lateral stacking pattern displayed by weakly amalgamated sheets in an increasingly confined basin plain setting. (A) Representative log and bed types of weakly amalgamated sheets (from Mt. Ramaceto F section; see Fig. 13). (B) Correlation panels (about 1.5 km wide) of weakly amalgamated sheets in the Mt. Ramaceto area showing consistency in bed package thickness but the poor correlatability of individual beds. The upward reduction in the lenticularity of individual beds is interpreted to reflect the increased confinement of the system.

Fig. 15. "Confined basin plain isolated sheet" facies and bed stacking pattern. (A) Representative log and bed types of Gottero confined basin plain deposits (from Mt. Ramaceto C section; see Fig. 13). (B) Landscape view of event beds in the Gottero 3 Mt. Ramaceto succession (note inversion of beds) including a mudstone clast rich (HEB-3) and chaotic HEBs (HEB-2) with thick mudstone caps and interbedded with hybrid-devoid, thin-bedded packages. (C) HEB-1 bed including heterolitic thin-bedded substrate rafts enclosed in the H3 division. (D) HEB-3 bed including relatively thin H1 sandy base with irregular top, a relatively abrupt transition into a mudstone-clast rich H3 division, and a thin draping laminated H4. Way-up is indicated by arrows and by b (base) and t (top) labels.

Fig. 16. Detailed cross-sections of selected intervals of the Gottero Sandstone succession in the Mt. Ramaceto area confirming the generally tabular geometry and correlativity of individual beds at km-scale albeit with local erosion of hybrid event beds into the substrate. The distances between the different logs are indicative only, because of the variable angle between them. (A) Panel A representing the succession between 120 m and 177 m from the stratigraphic top of the Gottero formation in Mt. Ramaceto area (see Fig. 13); (B) Panel B shows the succession between 260 m and 354 m from the stratigraphic top. The two panels capture a large-scale stratigraphic trend in which single event beds are increasingly separated by mudstone intervals towards the uppermost

part of the succession interpreted as effect of progressive increase in the degree of confinement of the distal Gottero depocentre.

Fig. 17. Examples of observed facies tracts of mudstone-clast and raft-bearing HEBs from the Mt. Ramaceto succession. The letters refers to the section measured (see their location and context on Fig. 13). (A) Example of Type 1 facies tract (FTH-1) showing a longitudinal/lateral transition from a clean massive turbidite sandstone (section C) by enrichment and concentration of mudstone clasts (MRB – section E) and development of an HEB-3 (section G). The lateral transition is recorded also in the vertical bed profile of section G by the presence of a mudstone-clast rich H1b interval beneath the H3 division of the bed. Shallow scours (about 30 cm deep) are detected in section C, providing a possible source of mudstone clasts from the underlying substrate. (B) Examples of Type 2 facies tract (FTH-2) showing that in section A, where the degree of substrate removal is at a maximum, the event bed includes large substrate rafts within the H3 division, characterised by preserved thin-bedded stratigraphy (HEB-1). Proceeding through the more distal sections the substrate rafts are progressively destroyed and the texture of the H3 division became a mudstone clast-rich debrite (MCB - HEB-3) but with some pieces of chaotic material still preserved (HEB-2). In both cases the thickness of the H4 division is similar throughout the entire facies tract.

Fig. 18. Hybrid event bed facies tracts detected in the Gottero system. All of them show a downcurrent and lateral transition from relatively clean high-density turbidite (HDT) to a hybrid event bed (HEB) due to abundant mud clast incorporation. (A) FTH-1 is characterised by a very strong lateral relationship between mudstone clast-rich but relatively clean sandstone beds (MRBs) and hybrid event beds with mud clast-rich H3 divisions (HEB-3). This lateral facies association is linked to elongated shallow scours. (B) FTH-2 shows a downcurrent and lateral passages between a large raft-bearing HEB (HEB-1) and a different kind of strongly injected/chaotic (HEB-2) or mudstone clast-rich HEB (HEB-3). In this case the beds are associated with large deep scours where substrate blocks were locally detached from the sea-floor and incorporated into the flow. (C) FTH-3 predicts a downflow/lateral transformation from clean high-density turbidites to thin hybrid

event beds that may include a banded division (H2). The down-dip transition occurs from beds with thin H3 divisions to beds with an expanded H3. The mud entrainment can be provided in form of loose clay and small mud chips, by turbulent erosion in up-dip locations.

Fig. 19. Sketch summarising the stratigraphic distribution, character and typical stacking pattern of hybrid event beds in fan and basin plain settings, based on the Gottero example. (1) Unconfined fan systems are generally devoid of hybrid event beds in their proximal area, developing HEBs preferentially in the fan fringe and at the base of thickening upward lobe sequences. HEBs are characteristically thin and belong to types 5 and 6. HEBs 1 to 4 can be occasionally found directly above mud-prone inter-lobe deposits. (2) In confined basin plain successions developed in tectonically active basins characterised by flat basin floor topography, the sedimentation is dominated by high-volume flows able to delaminate the substrate and develop thick mudstone clast or raft-bearing HEBs (HEB-1 to 4).

Tab. 1. Description and interpretation of bed type classes distinguished in the present study.

Tab. 2. Hybrid event bed character statistical summary.

Bed type class	Description	Interpretation
Debrites (DEBs)	Matrix-supported poorly sorted conglomerates and muddy sandstones	Deposited by cohesive debris flows whose larger clasts are supported by a cohesive clay-rich matrix (Pierson, 1981; Mulder and Alexander, 2001; Mohrig & Marr, 2003)
Gravelly high-density turbidites (GHDTs)	Clast-supported conglomerates and pebbly sandstones found as either isolated deposits or at the base of thick graded beds. They can be distinguished as: i) mudstone-clast conglomerates; ii) conglomeratic-lag lenses and iii) pebbles and granules in planar to cross-laminated sandstones.	Deposited by hyperconcentrated flow – i.e. non-Newtonian but non-plastic flows with high shear strength and intermediate rheology between cohesive and fluidal flows; sediment was supported by a combination of turbulence, dispersive pressure and buoyancy (Costa, 1984; Smith, 1986; Mutti, 1992; Mulder & Alexander, 2001). When hyperconcentrated flows undergo flow transformation to a high-density turbidity current, they deposit lenticular conglomeratic lags because of the progressive loss of flow strength (Mutti, 1992) and can be reworked by the overlying flow forming dunes.
High-density turbidites (HDTs)	Beds including coarse (occasionally granule grade) to medium sand grade bases, eventually grading into or being overlain by finer facies. Bed bases can be characterised by structureless normally graded or ungraded sandstone, inverse graded intervals characterised by granules or coarse sand alignments. More rarely coarse-grained medium scale cross-laminations both as single sets and as a component facies are present.	Beds related to the rapid or progressive (e.g. layer-by-layer) deposition of high-concentration turbidity currents and by the reworking or suspension fall-out of the low-concentration turbulent flow tail (Lowe, 1982; Mutti, 1992; Kneller and Branney, 1995; Mulder & Alexander, 2001).
Mudstone-clast rich beds (MRBs)	Beds composed by a basal structureless sandstone and an uppermost structured and finer-grained division, sandwiching an interval enriched in mudstone clasts. Mudstone clasts are preferentially accumulated at the interface between the basal structureless and coarser-grain sandstone and the overlying finer-grained structured division. Occasionally larger mudstone clasts can be armoured by granules and pebbles in distinctive coarse-grained poorly sorted and massive beds. In the distal confined part of the system they are often found in close spatial relationship in the same event with mudstone clast-rich hybrid event beds.	Beds deposited by high-concentration turbidity currents and eventually capped by their associated low-concentration turbulent flow tails. The presence of abundant intra-formational mudstone clasts suggests that the flows were highly erosive at some stage during their runout and were able to detach and incorporate substrate pieces of variable size. The lateral transitions between MRBs and HEBs suggests the former can be interpreted as deposits of flows during the early stages of hybrid flow development (Fonnesu et al., 2015; Southern et al., 2015).
Hybrid event beds (HEBs)	Bipartite or tripartite beds constituted by a basal massive to crude laminated sandstone overlain by an argillaceous generally poorly sorted but texturally very variable sandstone, often rich in mudstone clasts and sheared sand patches. A fine/very fine-grained parallel to ripple laminated division graded into a silty to mudstone cap is eventually present at the top of the sequence.	Deposition from high-density turbidity currents enriched in mud by erosion of substrate or being already mud enriched, and underwent different degree of flow partitioning (Haughton et al., 2009; Kane & Pontén, 2012; Talling, 2013; Fonnesu et al., 2015; 2016). (See text).
Low-density turbidites (LDTs)	Generally thin, rippled, wavy to horizontally parallel laminated, fine-grained graded beds.	Product of low-concentration turbidity currents. They can be the deposit of smaller-volume flows or the distal expression of high-density (or hybrid; see Amy and Talling, 2006; Muzzi Magalhaes & Tinterri, 2010; Fonnesu et al., 2015) sediment flows that have already deposited the majority of their sediment load in more proximal or adjacent regions.
Limestone beds (L)	Calcarenitic to micritic, structureless to planar or wavy laminated beds grading into marls found as continuous or in nodular layers.	Limestone beds record deposition from rare calcareous turbidity currents (Marini, 1994). Some nodule layers could be of early diagenetic origin.

	HEB-1	HEB-2	HEB-3	HEB-4	HEB-5	HEB-6
Nº of beds (%)	32 (10.7%)	33 (11%)	129 (43%)	55 (18.3%)	46 (15.3%)	5 (1.7%)
Tot thickn. (%)	86.6 m (18.6%)	78.3 m (16.9%)	228 m (49.1%)	50.3 m (10.8%)	20.4 m (4.4%)	1.02 m (0.2%)
Max sandst. thickness	6.80 m	9.57 m	5.30 m	3.20 m	2.40 m	0.75 m
Min sandst. thickness	0.40 m	0.40 m	0.30 m	0.20 m	0.05 m	0.12 m
Aver. sandst. thickness	3.32 m	2.37 m	1.77 m	0.92 m	0.44 m	0.20 m
Aver. thickn. of H1+H1b	0.96 m	0.77 m	0.81 m	0.38 m	0.17 m	
Aver. thickn. of H3	1.37 m	1.27 m	0.72 m	0.39 m	0.23 m	0.10 m
Presence of H4 (%)	30 (94%)	26 (79%)	112 (87%)	45 (82%)	22 (48%)	
Aver. thickn. of H4	0.32 m	0.35 m	0.24 m	0.15 m	0.09 m	0.10 m

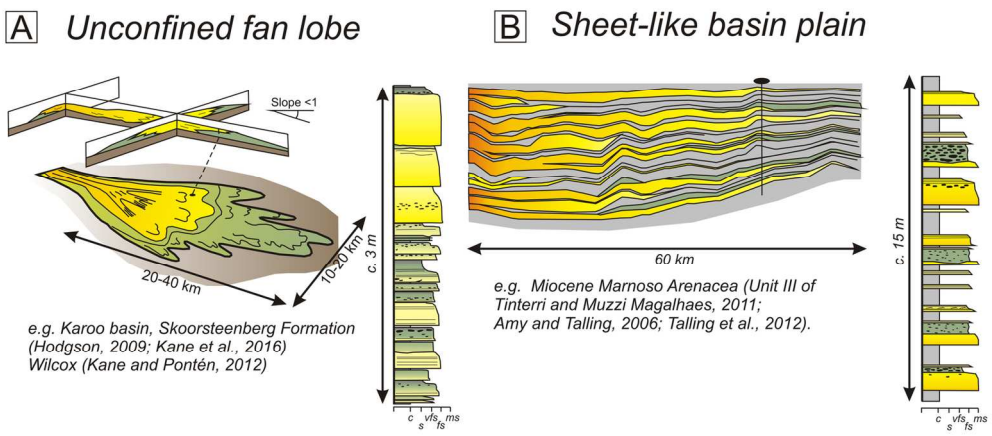

Fig. 1. Different styles of hybrid event bed distribution in turbidite systems, based on published examples. (A) Hybrid event beds in distributive lobe systems (modified from Hodgson, 2009) and their vertical arrangement in 1D logs at the base of prograding lobes (Kane & Pontén, 2012). (B) Hybrid event beds in confined basin plains (based on stratigraphic cross-section of Unit 3 of Miocene Marnoso-arenacea Formation, sensu Tinterri and Muzzi Magalhes, 2011, from Talling et al., 2012 in the interval below the Contessa key bed); the synthetic vertical log shows the lack of vertical organization of hybrid event beds and conventional turbidites at c. 20 m scale.

73x32mm (600 x 600 DPI)

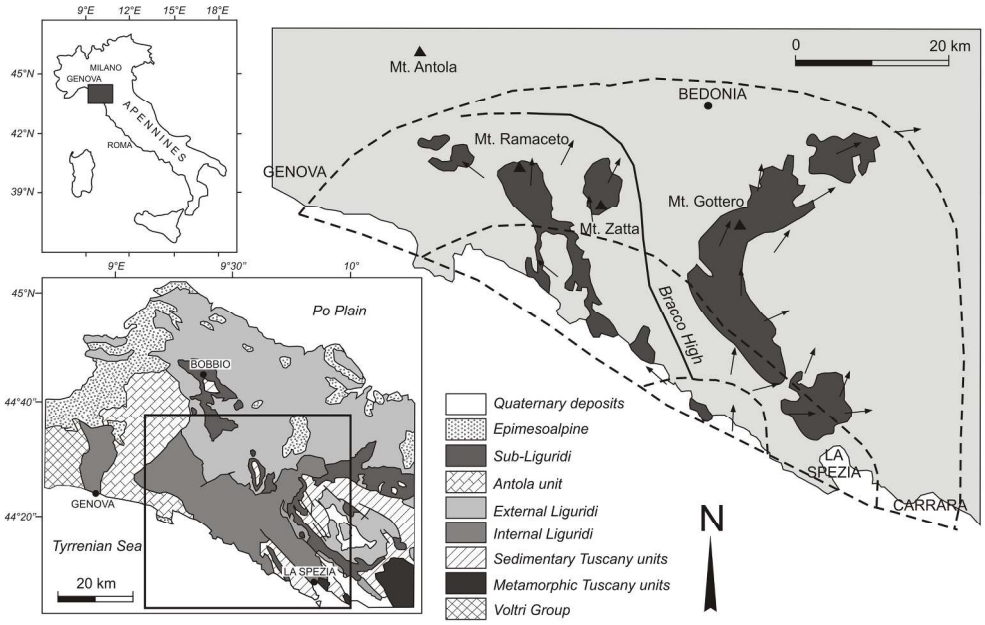

Fig. 2. - Location map of the Gottero system (modified from Nilsen & Abbate, 1984) and sketch map showing the tectonic units of the Northern Apennines (modified from Elter et al., 1992). The arrows in the location map indicate the main palaeocurrent pattern deduced by Nilsen & Abbate (1984).

107x67mm (600 x 600 DPI)

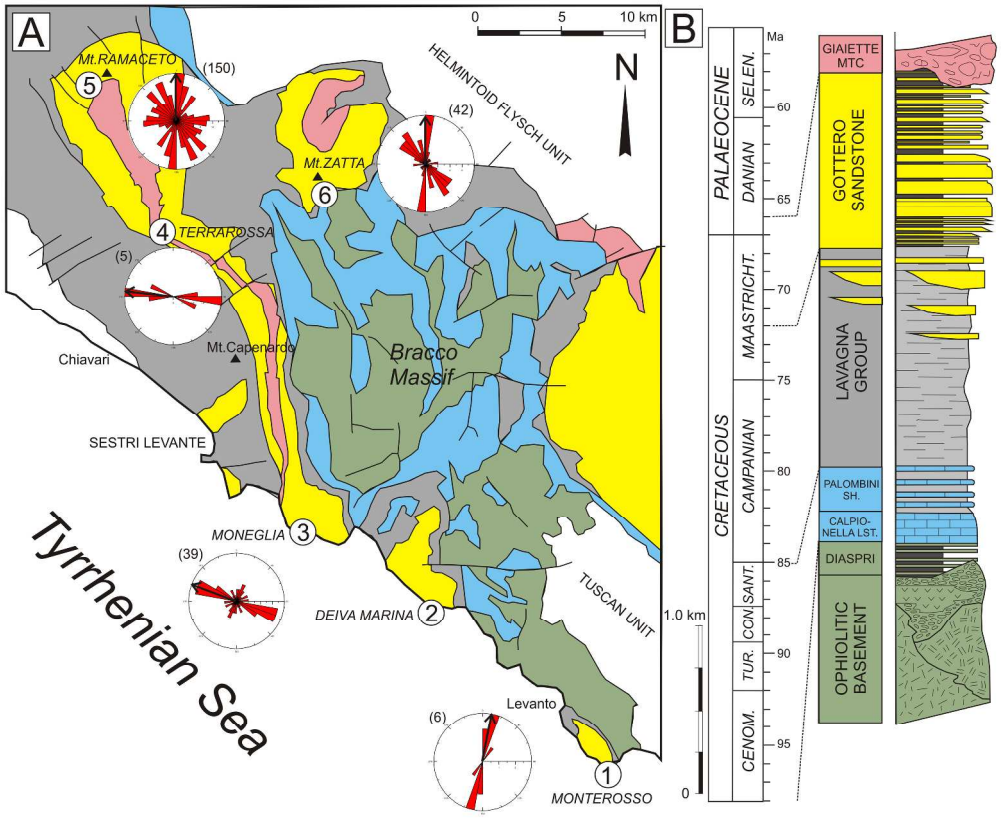

Fig. 3. (A) Simplified geological map of the Western Gottero study area (modified from Marroni, 1994) showing the location of measured sections (1 to 6) and palaeocurrent roses obtained during this study; the numbers in brackets indicate the number of palaeocurrent measurements. The palaeoflow pattern broadly corresponds to that established by Nilsen & Abbate (1984) (see Fig. 2). (B) Internal Liguridi stratigraphy of the Gottero tectonic unit (modified from Marroni et al., 2001). The colours on the map correspond to those displayed in the stratigraphic log.

140x115mm (600 x 600 DPI)

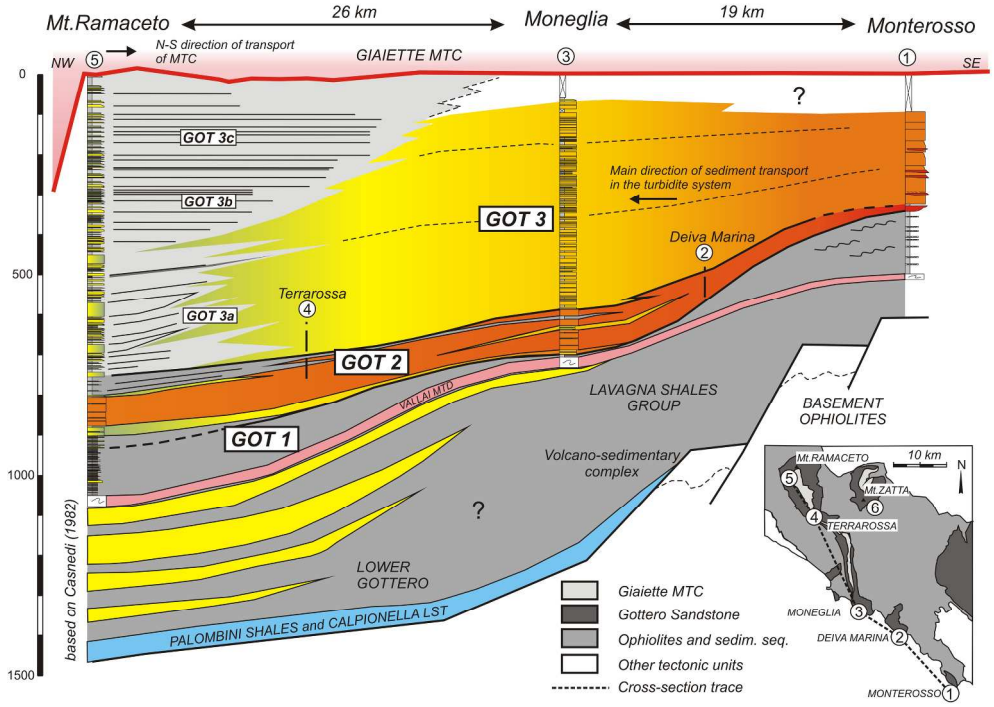

Fig. 4. General NW-SE cross-section of the Gottero system aligned in a direction approximately parallel to the sediment transport. Colour shading according to the major grain-size and lithofacies (red colours: conglomerate and coarse grained sandstones, green: hybrid event beds, grey: mostly siltstone and mudstones or fine-grained sandstones, pink: mass transport complexes). The area interpreted as confined basin plain is coloured in light grey on the correlation panel. Note the distances between sections have not been palinspastically restored and could potentially be longer than indicated.

123x89mm (600 x 600 DPI)

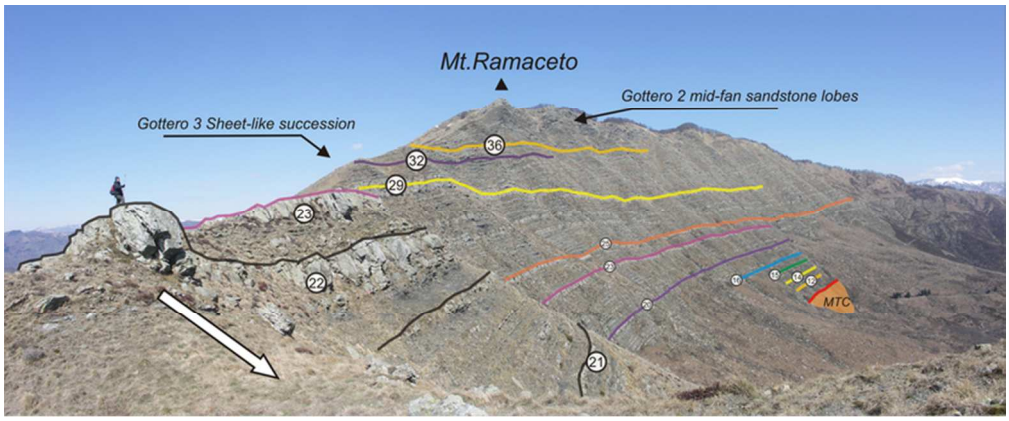

Fig. 5. Exposure of the upper stratigraphic part of the Gottero Sandstone in the Mt. Ramaceto area. Note the succession is tectonically inverted (arrow indicates succession way-up). Numbers refer to photohorizons highlighted in the correlation panel of Fig. 13. Orange colour represents the outcrop of the stratigraphically overlying Giaiette mass transport complex unit (MTC). The picture capture about 2.2 km lateral exposure and 740 m of stratigraphic thickness.

69x28mm (300 x 300 DPI)

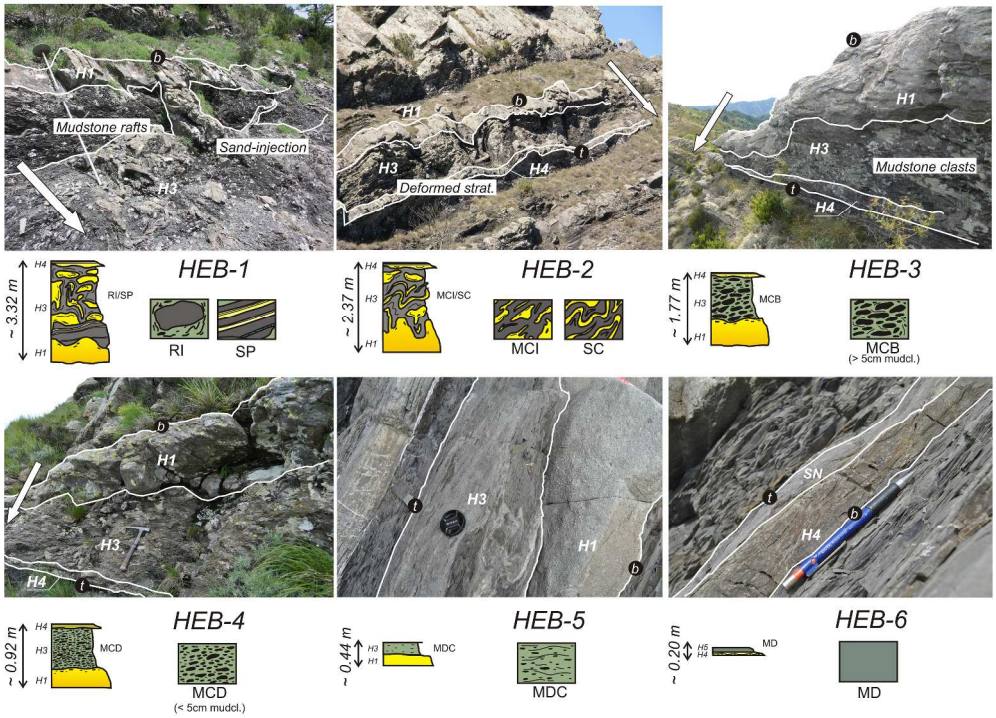

Fig. 6. Hybrid event bed classification scheme. Typical bed profiles (with average bed thicknesses) and photo examples. Arrows indicate the way-up when bedding is inverted (b, base of the bed; t, top of the bed).. Typical H3 sub-facies are indicated in the boxes. HEB-1 and HEB-2 can contain H3 divisions of two types: RI and MCI sub-facies can be made of undeformed or deformed mudstone rafts; SP and SC sub-facies can include undeformed pieces of thin-bedded stratigraphy or their deformed equivalents respectively. MCB: densely packed mudstone clasts (average over 5 cm) surrounded by dirty sandstone; MCD: small (2-5 cm) mudstone clasts in a dirty sandstone matrix; MDC: argillaceous sandstone with scatter mudstone clasts; MD: argillaceous sandstone without mud-chips.

169x125mm (600 x 600 DPI)

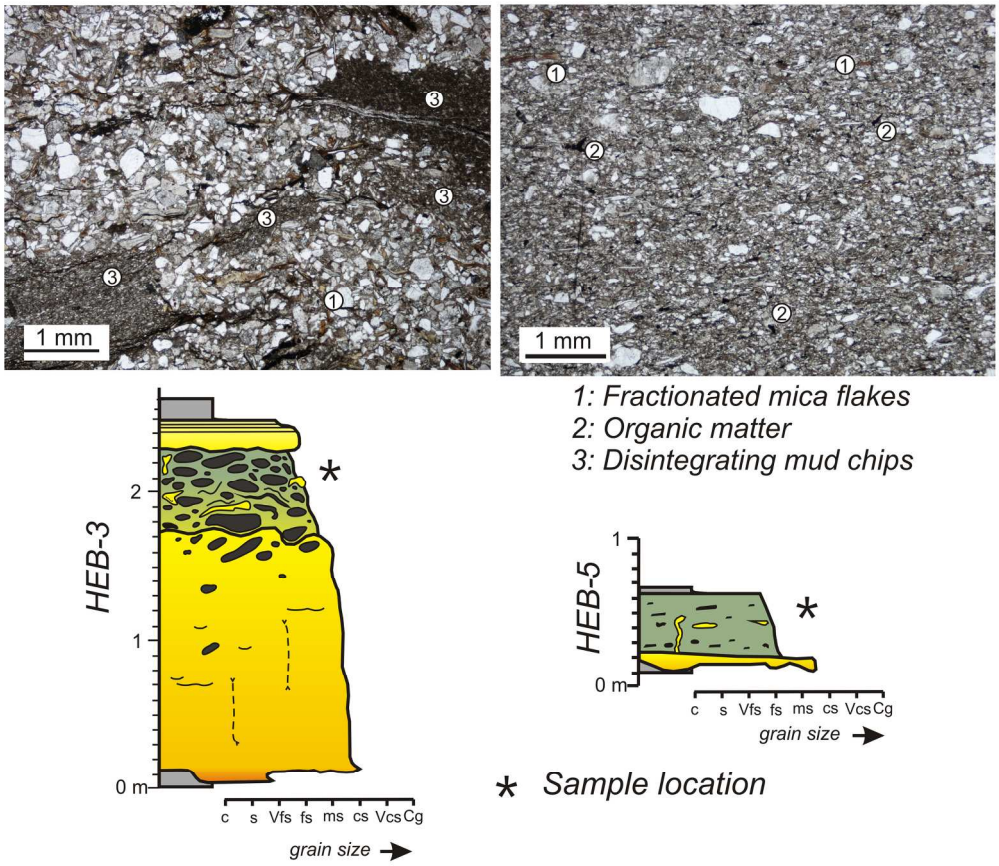

Fig. 7. Petrographic and textural characteristics of the H3 division in the Gottero hybrid event beds. Samples are from HEB-3 and HEB-5 event beds located in Mt. Ramaceto and Moneglia sections respectively. The dispersed clay content (counted 500 points per section) reaches 20% in the first sample and 27% in the latter. In the HEB-3 sample mud chips are captured in the act of being partially disaggregated and contributing mud to the matrix.

97x84mm (600 x 600 DPI)

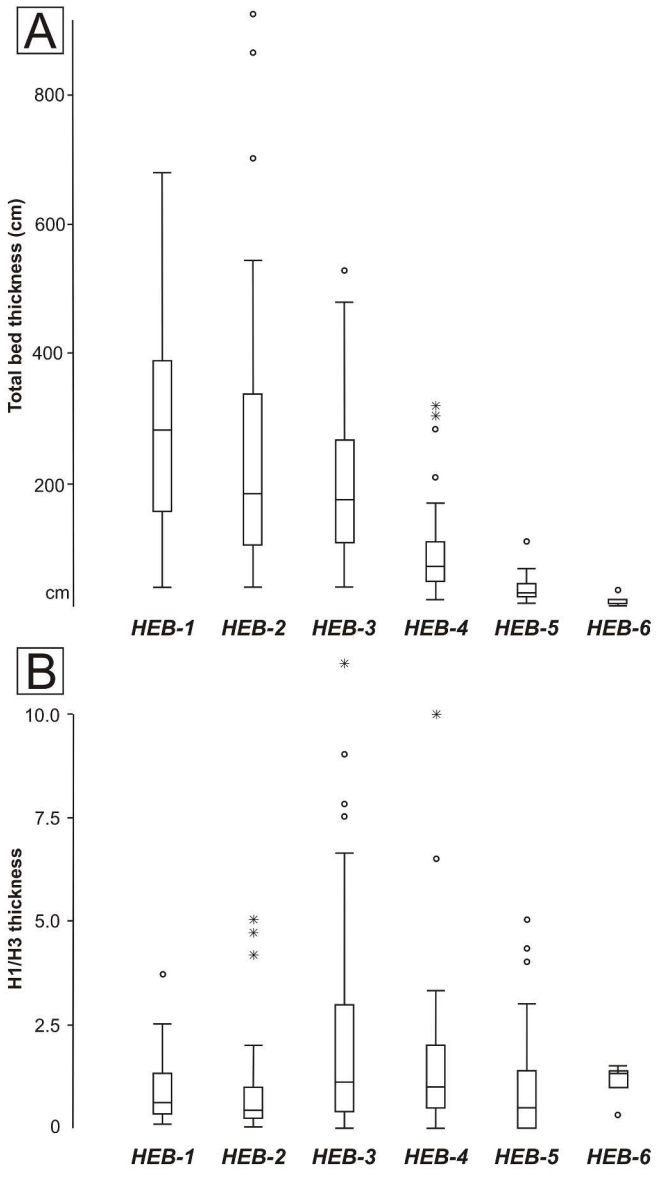

Fig. 8. Thickness characteristics of hybrid event beds. (A) Box-plot showing the direct correlation between average, maximum and minimum thickness of the sandy portion (H1 to H4) of the bed, and the type of hybrid event bed. (B) Box-plot displaying the lack of correlation between the hybrid event bed type and the H1/H3 ratio, HEB-3s have the higher variability.

138x238mm (600 x 600 DPI)

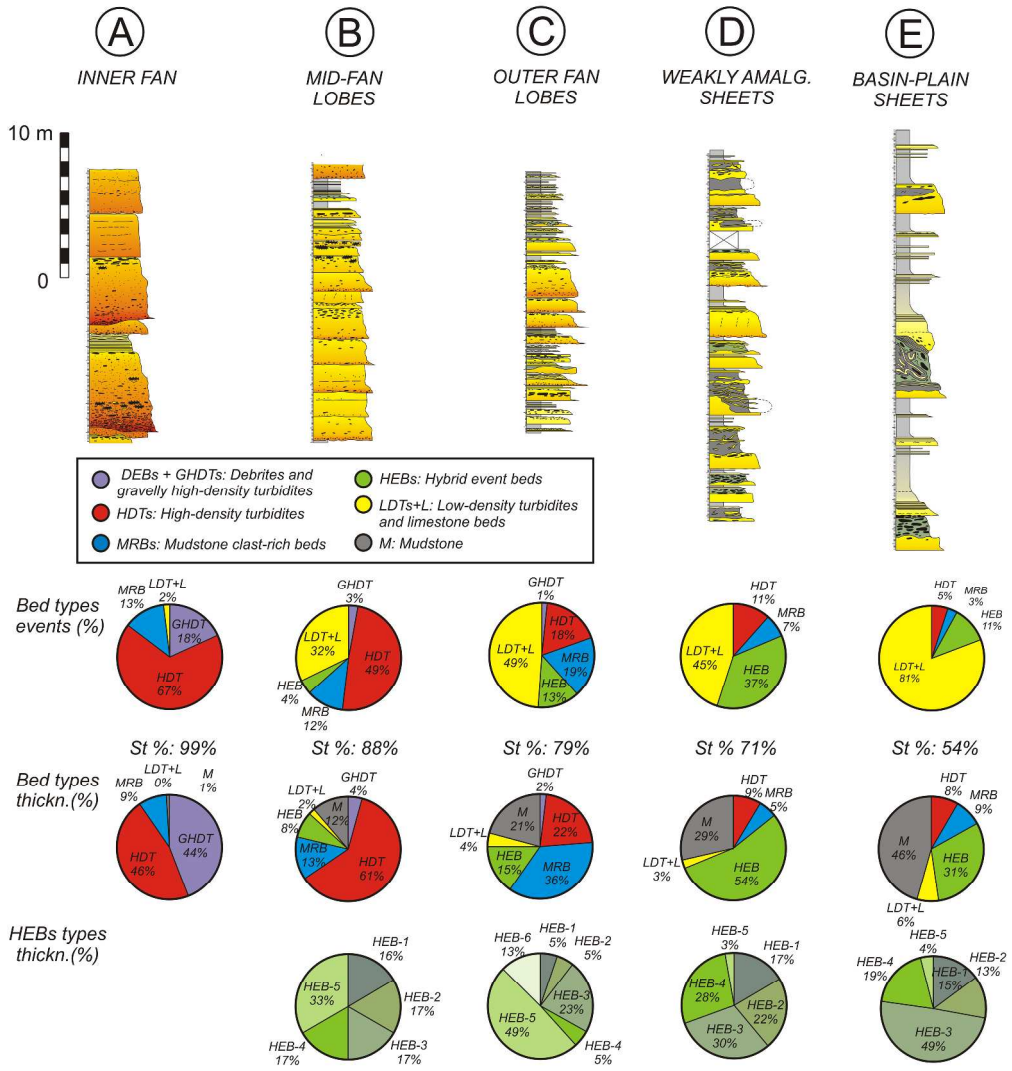

Fig. 9. Sandy facies associations and related interpreted depositional environments identified in the Gottero Sandstone and event bed percentages. Sedimentological logs represent examples of stacking patterns for each facies association. Pie charts show the relative abundance of bed types (for number of events and in thickness) and hybrid event bed types for each facies association (in thickness). St%: sandstone percentage of the facies association. Debrites (DEBs) and gravelly high-density turbidites (GHDTs), and low-density turbidites (LDTs) and limestones (L) categories are merged together in the statistics.

183x198mm (600 x 600 DPI)

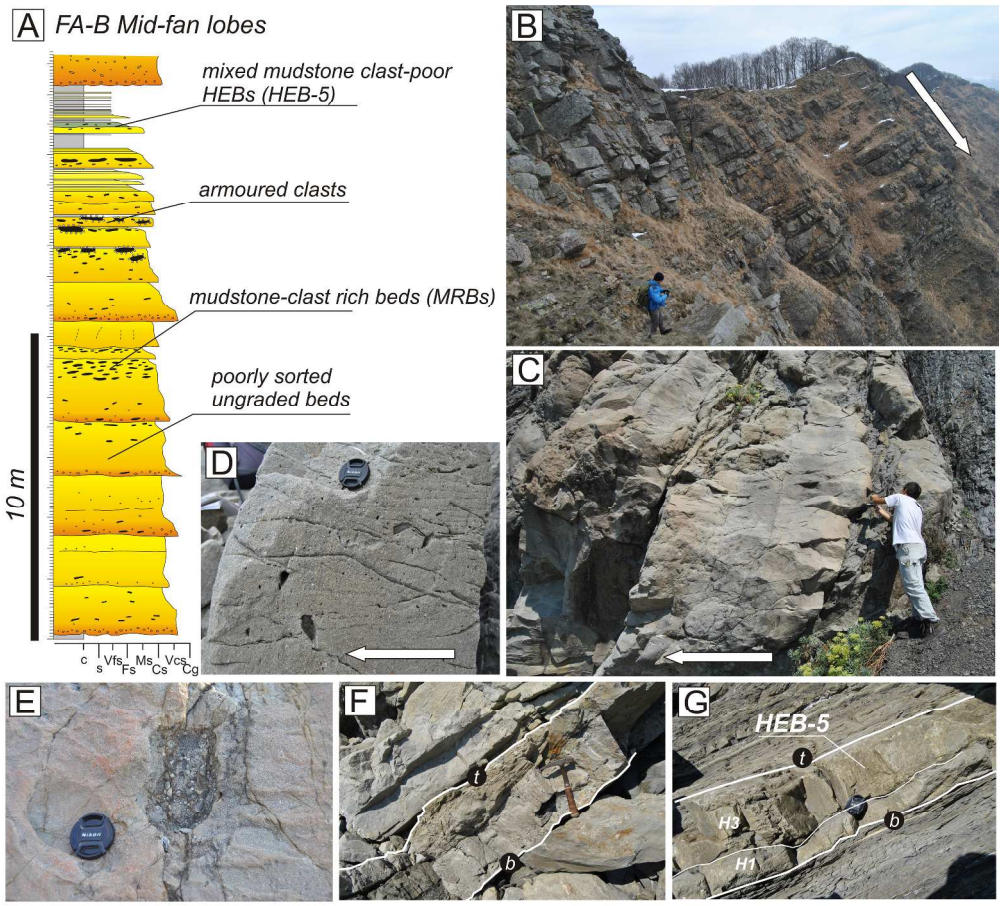

Fig. 10. Mid-fan amalgamated lobe facies and stacking patterns. (A) Representative log and typical bed types of Gottero mid-fan amalgamated lobe deposits (from the Moneglia locality, see location in Fig. 3). (B) Gottero 2 mid-fan lobes in the Mt. Ramaceto section: despite being grouped in the same facies association, the beds are slightly less amalgamated and finer grained than in the Moneglia or Deiva Marina examples. (C) Amalgamated coarse-grained sandstone beds in Moneglia showing slightly erosive bases on the underlying deposits. (D) Poorly sorted coarse-grained bed in Moneglia. (E) Granule-armoured mudstone clast. (F) Conglomeratic lenticular bed draped by fine-grained and rippled bed (Moneglia). (G) Thin and fine-grained HEB-5 bed in mud-prone inter-lobe deposits. Way-up is indicated by arrows and by b (base) and t (top) labels.

154x141mm (600 x 600 DPI)

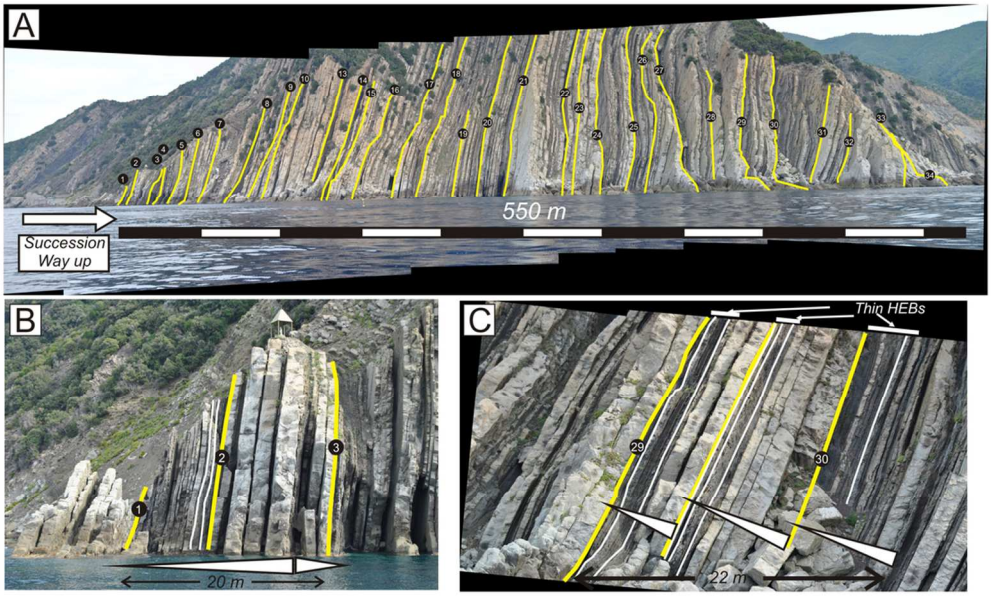

Fig. 11. Outer-fan lobe architecture in Moneglia (Punta Baffe locality). (A) Cliff exposure of Gottero 3 sandstone; numbers represent surfaces across which changes in stacking pattern occur. (B) Close-up of the logged section displaying a 20 m thick thickening and thinning cycle. (C) Three smaller-scale thickening upward cycles in the intermediate part of the section in which thin HEBs are concentrated at the bases. Way-up to the right in B and C. Bed thickness trends are indicated by triangles.

101x61mm (300 x 300 DPI)

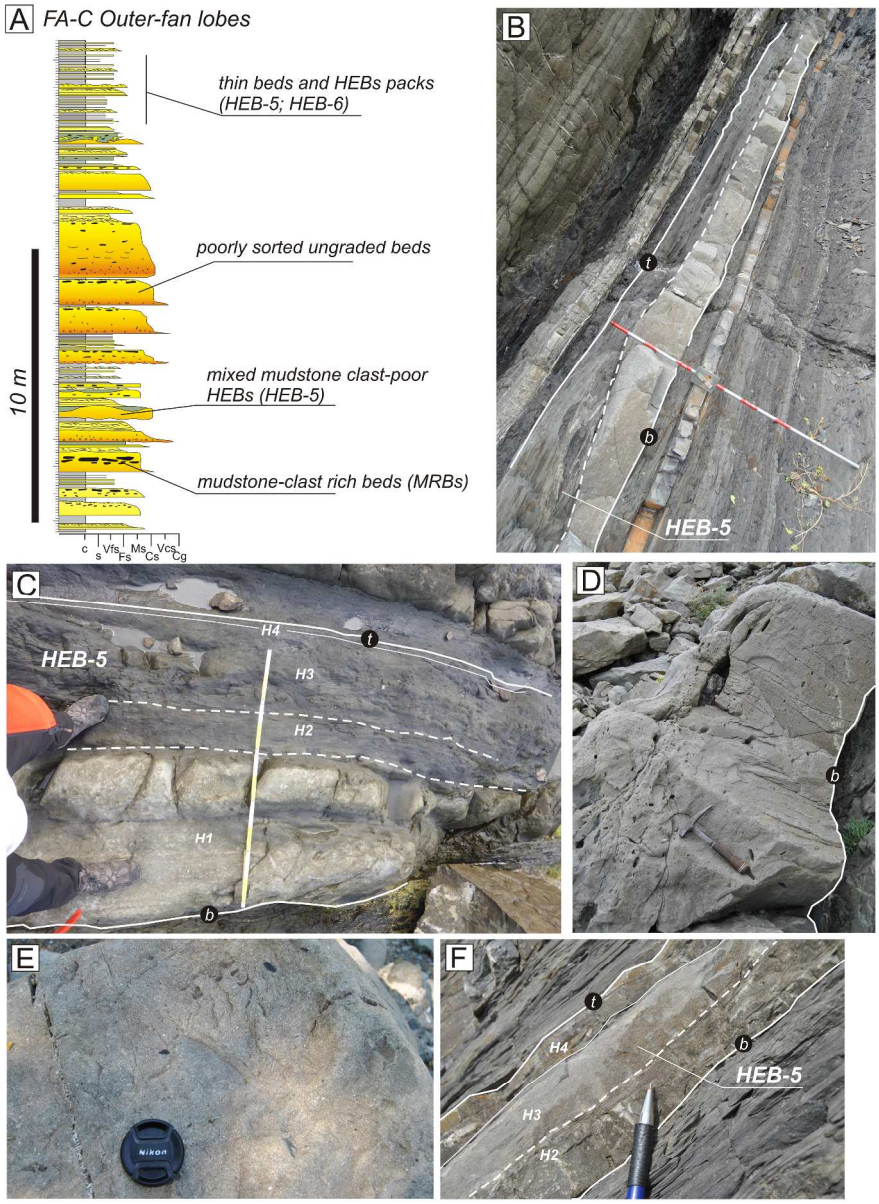

Fig. 12. Outer-fan lobes facies and related stacking pattern. (A) Representative log and bed types of the Gottero outer-fan lobes (from Moneglia locality, see location in Fig. 3). (B) Example of HEB-5 interbedded with thin-bedded lobe fringe deposit at the base of a lobe cycle. (C) HEB-5 including a well-developed H2 banded division. (D) Poorly sorted mudstone-clast rich bed (MRB) in Moneglia lobe deposits. (E) Poorly sorted coarse-sandstone texture with small scattered angular mudstone clasts (Terrarossa section; location in Fig. 3). (F) Thin HEB-5 bed interbedded in lobe fringe deposits including a thin H2 banded interval and a rippled H4 division. All beds examples are right way-up (b: base; t: top).

229x309mm (600 x 600 DPI)

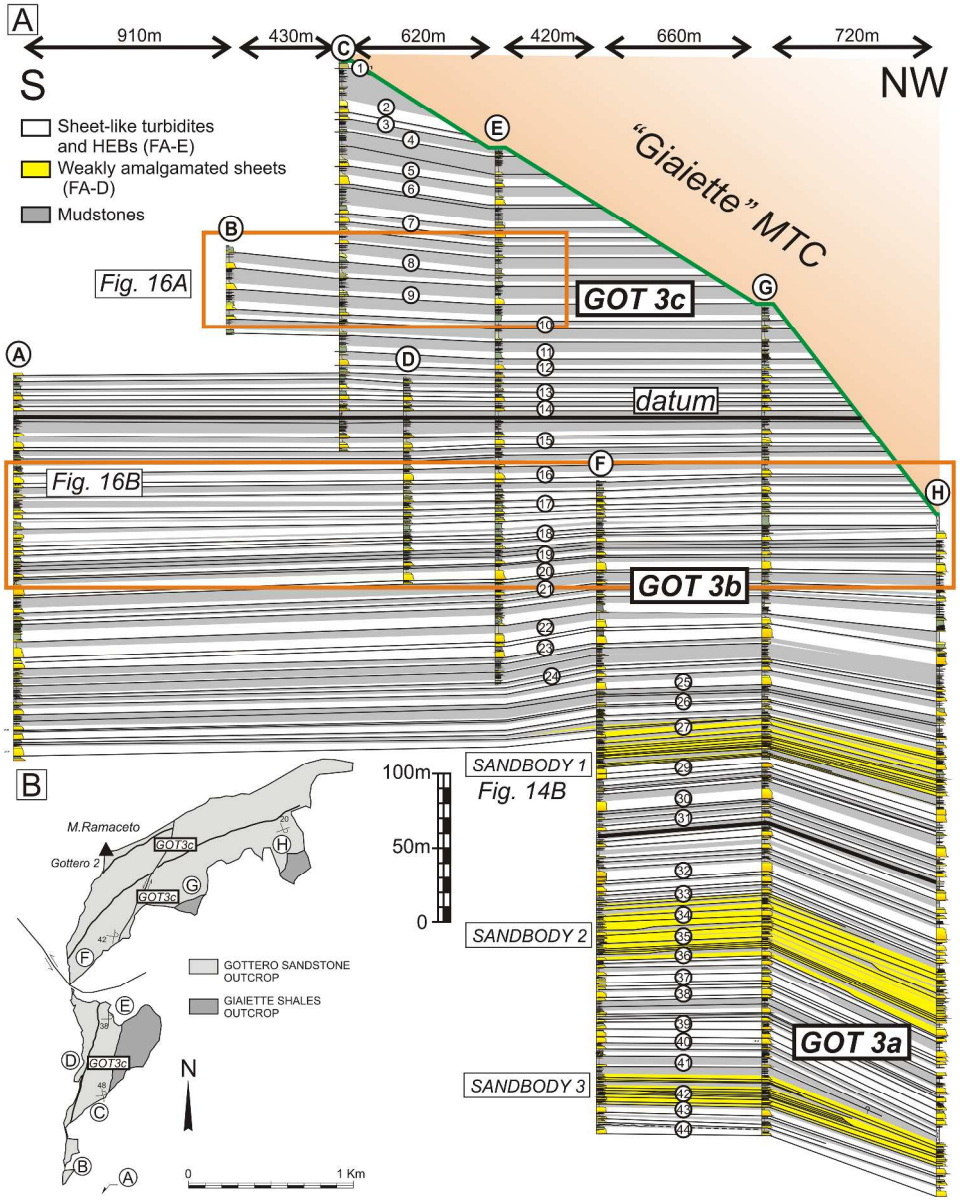

Fig. 13. Architecture and stacking pattern of the Gottero 3 succession in the Mt. Ramaceto area including FA-D and FA-E facies associations (modified from Fonnesu et al., 2013). (A) Correlation panel of the upper Gottero succession from eight logs spaced over 4 km laterally. The turbiditic succession is overlain by a >300 m thick chaotic level (Giaiette shales) emplaced by mass transport processes. The base of the mass transport complex records the erosion of more than 250 m of turbiditic succession over less than 2.5 km laterally. The numbers refer to the photohorizons shown in Fig. 5, and to other labelled beds. The datum is taken at a distinctive mud-prone level rich in diagenetic carbonate nodules ("Septarie lavel" of Andri and Zavatteri, 1990). Three units bounded by mud-prone intervals (Gottero 3a, 3b, 3c; GOT3a-3b-3c) are distinguished on the basis of a progressive upward increase of sedimentological characteristics indicating an increase in the degree of flow ponding (see text for details). Red boxes represent areas covered by the detailed correlation panels of Fig. 16. (B) Simplified outcrop map showing the position of the measured sections, the bed strikes and dips and the boundaries of the stratigraphic units.

213x267mm (600 x 600 DPI)

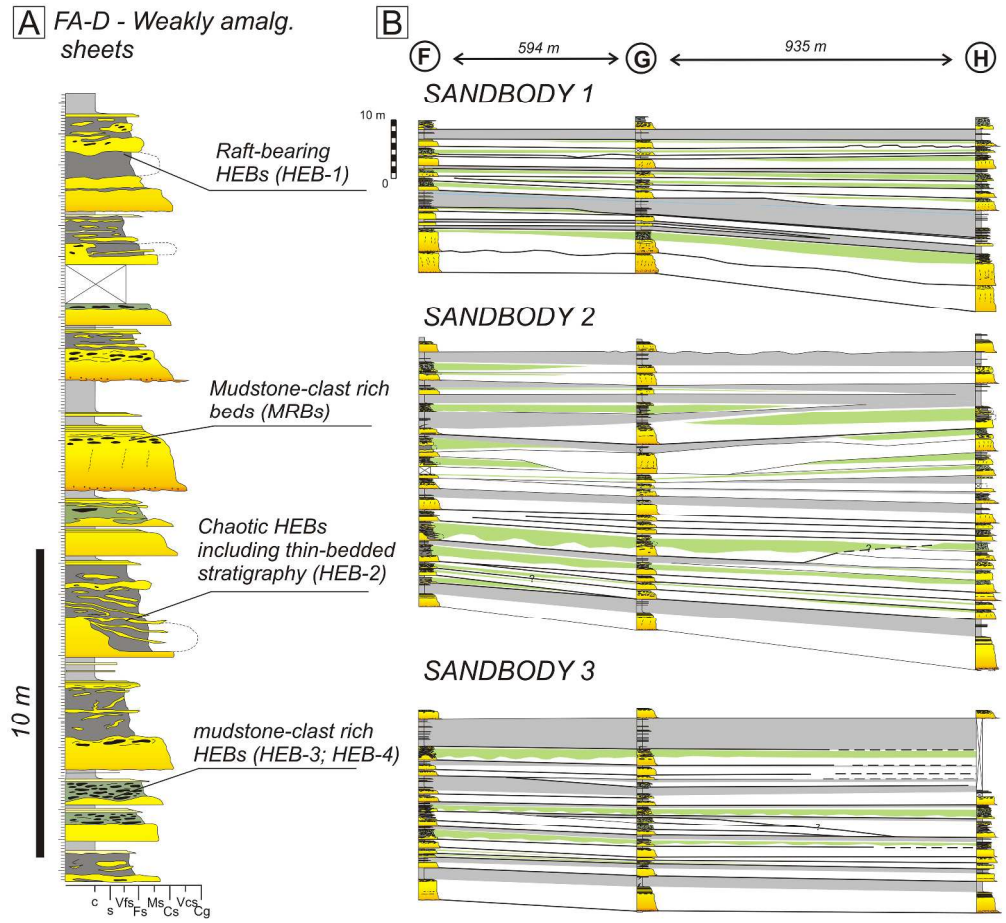

Fig. 14. Vertical and lateral stacking pattern displayed by weakly amalgamated sheets in an increasingly confined basin plain setting. (A) Representative log and bed types of weakly amalgamated sheets (from Mt. Ramaceto F section; see Fig. 13). (B) Correlation panels (about 1.5 km wide) of weakly amalgamated sheets in the Mt. Ramaceto area showing consistency in bed package thickness but the poor correlatability of individual beds. The upward reduction in the lenticularity of individual beds is interpreted to reflect the increased confinement of the system.

157x146mm (600 x 600 DPI)

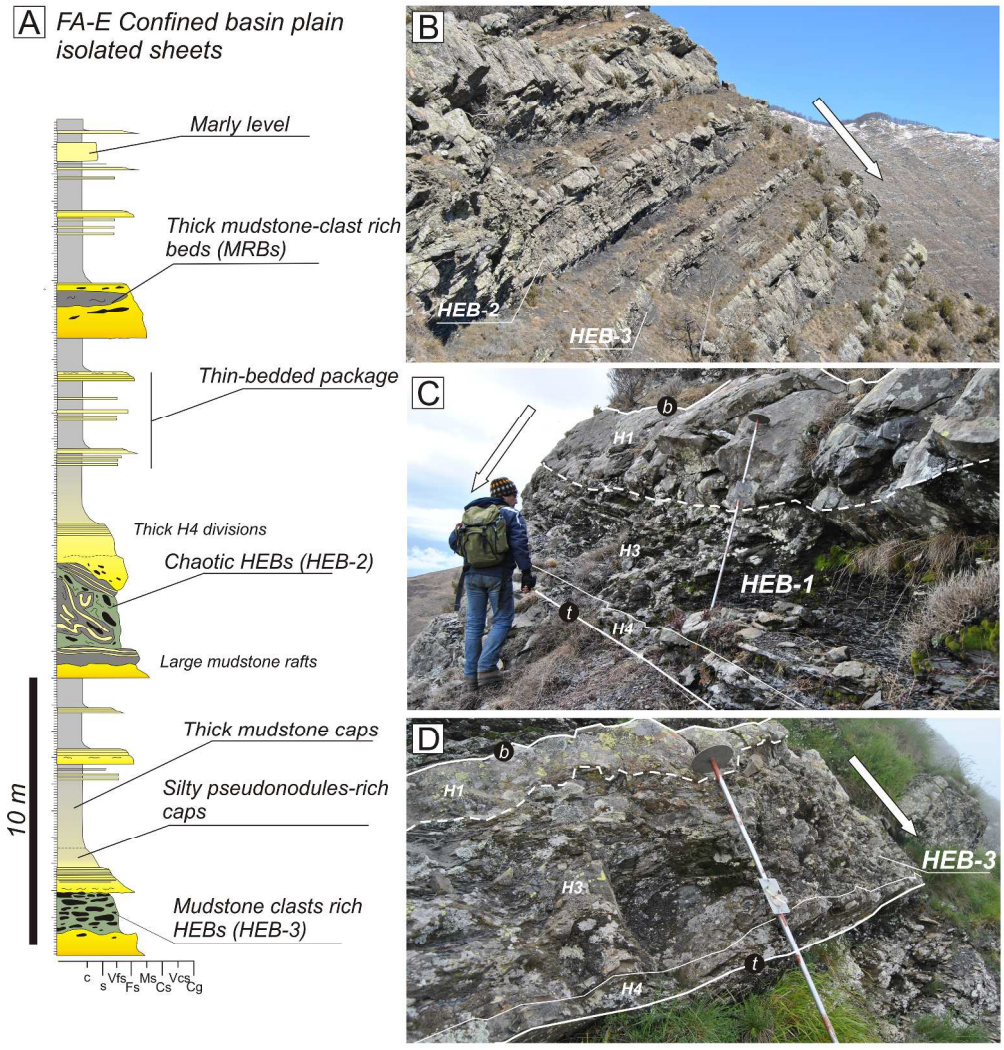

Fig. 15. "Confined basin plain isolated sheet" facies and bed stacking pattern. (A) Representative log and bed types of Gottero confined basin plain deposits (from Mt. Ramaceto C section; see Fig. 13). (B) Landscape view of event beds in the Gottero 3 Mt. Ramaceto succession (note inversion of beds) including a mudstone clast rich (HEB-3) and chaotic HEBs (HEB-2) with thick mudstone caps and interbedded with hybrid-devoid, thin-bedded packages. (C) HEB-1 bed including heterolitic thin-bedded substrate rafts enclosed in the H3 division. (D) HEB-3 bed including relatively thin H1 sandy base with irregular top, a relatively abrupt transition into a mudstone-clast rich H3 division, and a thin draping laminated H4. Way-up is indicated by arrows and by b (base) and t (top) labels.

178x187mm (600 x 600 DPI)

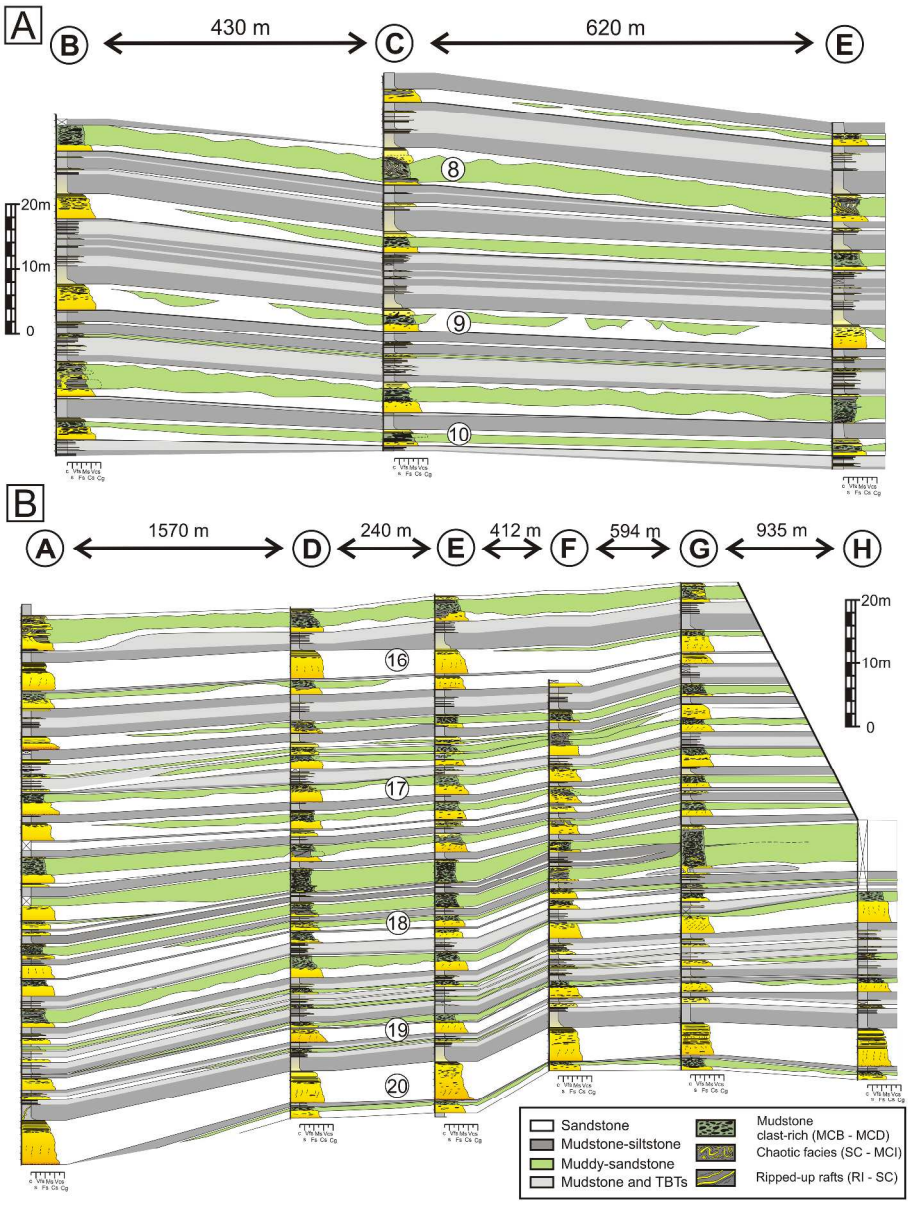

Fig. 16. Detailed cross-sections of selected intervals of the Gottero Sandstone succession in the Mt. Ramaceto area confirming the generally tabular geometry and correlativity of individual beds at km-scale albeit with local erosion of hybrid event beds into the substrate. The distances between the different logs are indicative only, because of the variable angle between them. (A) Panel A representing the succession between 120 m and 177 m from the stratigraphic top of the Gottero formation in Mt. Ramaceto area (see Fig. 13); (B) Panel B shows the succession between 260 m and 354 m from the stratigraphic top. The two panels capture a large-scale stratigraphic trend in which single event beds are increasingly separated by mudstone intervals towards the uppermost part of the succession interpreted as effect of progressive increase in the degree of confinement of the distal Gottero depocentre.

223x294mm (600 x 600 DPI)

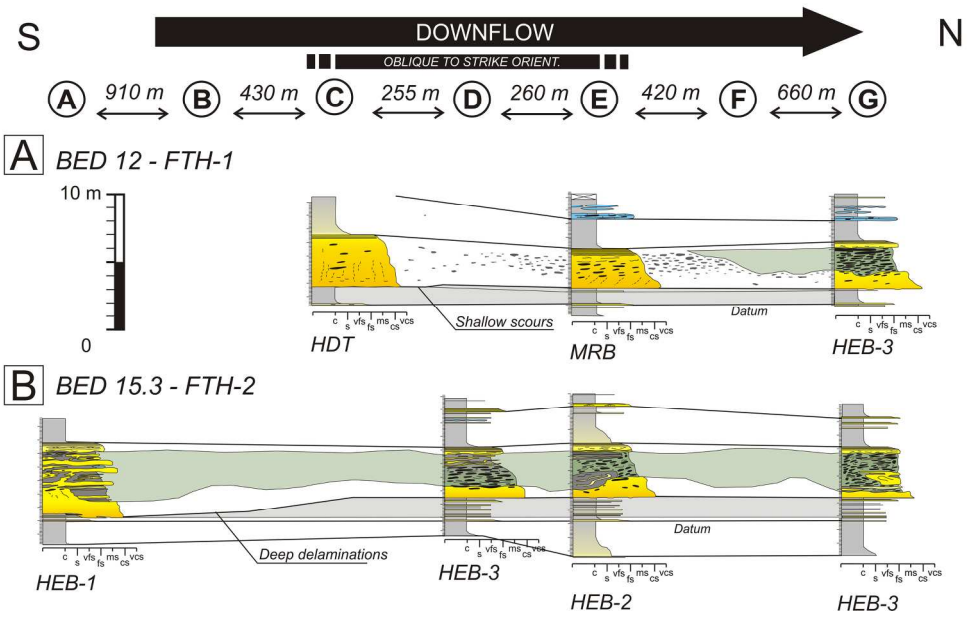

Fig. 17. Examples of observed facies tracts of mudstone-clast and raft-bearing HEBs from the Mt. Ramaceto succession. The letters refers to the section measured (see their location and context on Fig. 13). (A) Example of Type 1 facies tract (FTH-1) showing a longitudinal/lateral transition from a clean massive turbidite sandstone (section C) by enrichment and concentration of mudstone clasts (MRB – section E) and development of an HEB-3 (section G). The lateral transition is recorded also in the vertical bed profile of section G by the presence of a mudstone-clast rich H1b interval beneath the H3 division of the bed. Shallow scours (about 30 cm deep) are detected in section C, providing a possible source of mudstone clasts from the underlying substrate. (B) Examples of Type 2 facies tract (FTH-2) showing that in section A, where the degree of substrate removal is at a maximum, the event bed includes large substrate rafts within the H3 division, characterised by preserved thin-bedded stratigraphy (HEB-1). Proceeding through the more distal sections the substrate rafts are progressively destroyed and the texture of the H3 division became a mudstone clast-rich debrite (MCB - HEB-3) but with some pieces of chaotic material still preserved (HEB-2). In both cases the thickness of the H4 division is similar throughout the entire facies tract.

102x62mm (600 x 600 DPI)

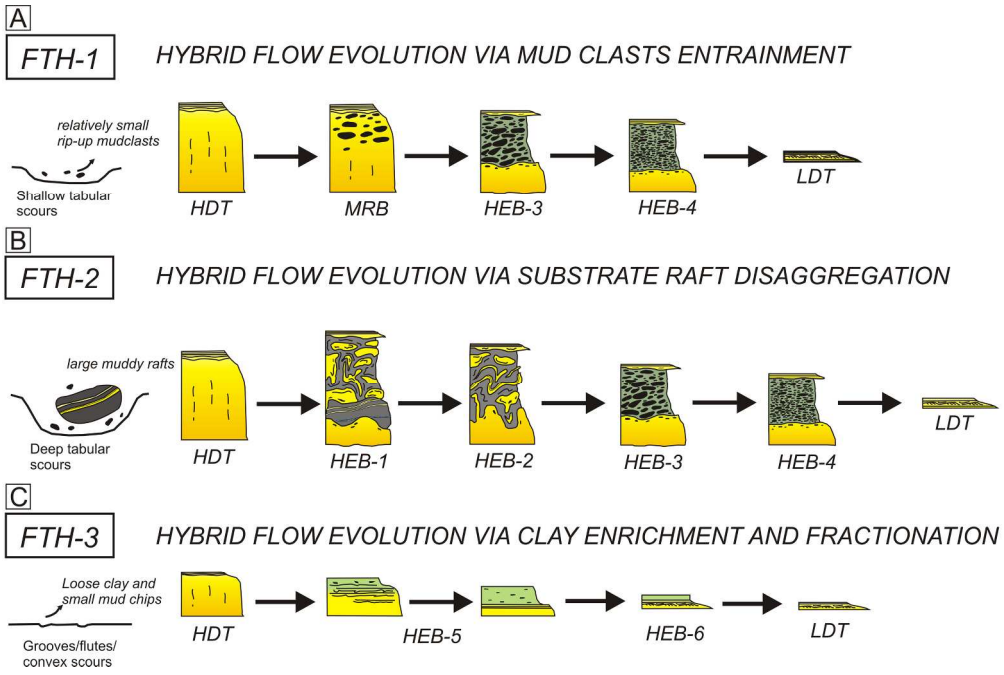

Fig. 18. Hybrid event bed facies tracts detected in the Gottero system. All of them show a downcurrent and lateral transition from relatively clean high-density turbidite (HDT) to a hybrid event bed (HEB) due to abundant mud clast incorporation. (A) FTH-1 is characterised by a very strong lateral relationship between mudstone clast-rich but relatively clean sandstone beds (MRBs) and hybrid event beds with mud clast-rich H3 divisions (HEB-3). This lateral facies association is linked to elongated shallow scours. (B) FTH-2 shows a downcurrent and lateral passages between a large raft-bearing HEB (HEB-1) and a different kind of strongly injected/chaotic (HEB-2) or mudstone clast-rich HEB (HEB-3). In this case the beds are associated with large deep scours where substrate blocks were locally detached from the sea-floor and incorporated into the flow. (C) FTH-3 predicts a downflow/lateral transformation from clean high-density turbidites to thin hybrid event beds that may include a banded division (H2). The down-dip transition occurs from beds with thin H3 divisions to beds with an expanded H3. The mud entrainment can be provided in form of loose clay and small mud chips, by turbulent erosion in up-dip locations.

112x74mm (600 x 600 DPI)

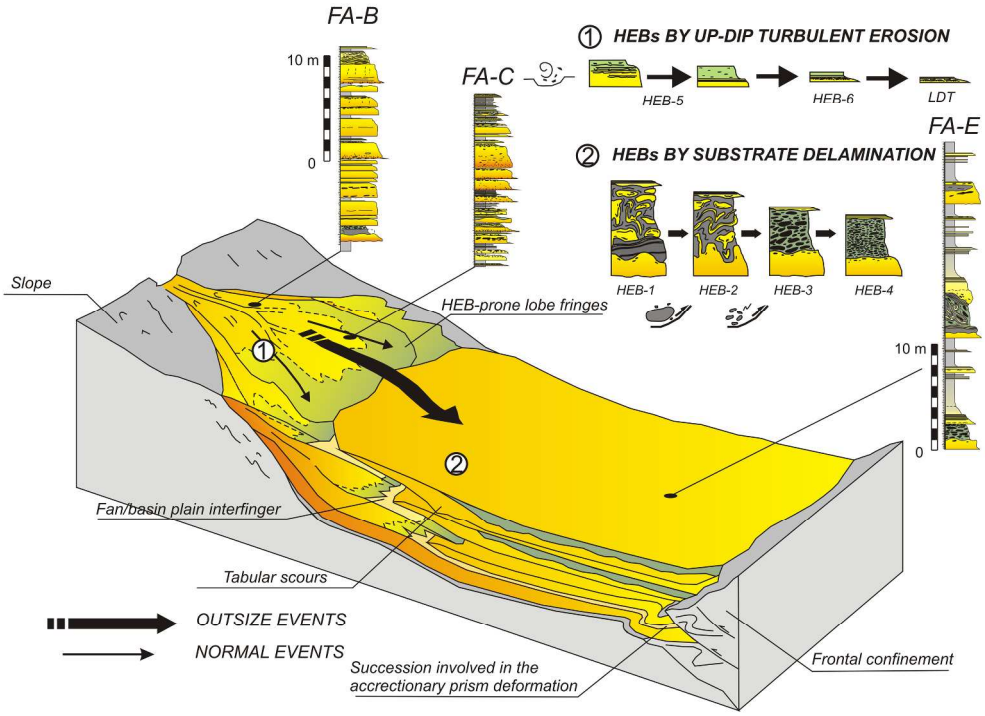

Fig. 19. Sketch summarising the stratigraphic distribution, character and typical stacking pattern of hybrid event beds in fan and basin plain settings, based on the Gottero example. (1) Unconfined fan systems are generally devoid of hybrid event beds in their proximal area, developing HEBs preferentially in the fan fringe and at the base of thickening upward lobe sequences. HEBs are characteristically thin and belong to types 5 and 6. HEBs 1 to 4 can be occasionally found directly above mud-prone inter-lobe deposits. (2) In confined basin plain successions developed in tectonically active basins characterised by flat basin floor topography, the sedimentation is dominated by high-volume flows able to delaminate the substrate and develop thick mudstone clast or raft-bearing HEBs (HEB-1 to 4).

123x90mm (600 x 600 DPI)